AFRL-PR-WP-TR-1998-2066

MISSILE FIN HEAT PIPE COOLING

BRIAN D. DONOVAN
WON S. CHANG
JOSEPH M. GOTTSCHLICH

POWER DIVISION
PROPULSION DIRECTORATE
AIR FORCE RESEARCH LABORATORY
WRIGHT-PATTERSON AFB OH 45433-7251

MAY 1998

FINAL REPORT FOR PERIOD JUNE 1, 1995 – JUNE 1, 1997

PROPULSION DIRECTORATE
AIR FORCE RESEARCH LABORATORY
AIR FORCE MATERIEL COMMAND
WRIGHT-PATTERSON AIR FORCE BASE, OH 45433-7251

NOTICE

USING GOVERNMENT DRAWINGS, SPECIFICATIONS, OR OTHER DATA INCLUDED IN THIS DOCUMENT FOR ANY PURPOSE OTHER THAN GOVERNMENT PROCUREMENT DOES NOT IN ANY WAY OBLIGATE THE US GOVERNMENT. THE FACT THAT THE GOVERNMENT FORMULATED OR SUPPLIED THE DRAWINGS, SPECIFICATIONS, OR OTHER DATA DOES NOT LICENSE THE HOLDER OR ANY OTHER PERSON OR CORPORATION; OR CONVEY ANY RIGHTS OR PERMISSION TO MANUFACTURE, USE, OR SELL ANY PATENTED INVENTION THAT MAY RELATE TO THEM.

THIS REPORT IS RELEASABLE TO THE NATIONAL TECHNICAL INFORMATION SERVICE (NTIS). AT NTIS, IT WILL BE AVAILABLE TO THE GENERAL PUBLIC, INCLUDING FOREIGN NATIONS.

THIS TECHNICAL REPORT HAS BEEN REVIEWED AND IS APPROVED FOR PUBLICATION.

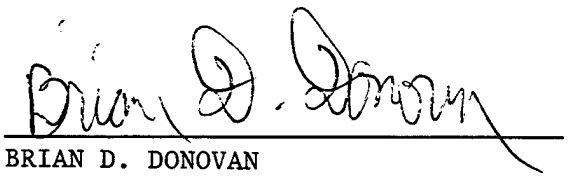

BRIAN D. DONOVAN
Project Engineer
Power Generation & Thermal
Management Branch
Power Division

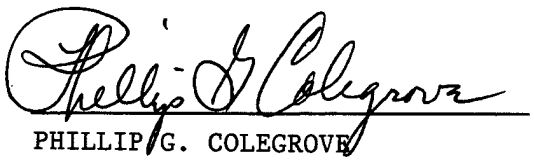

PHILLIP G. COLEGROVE
Chief, Power Generation & Thermal
Management Branch
Power Division

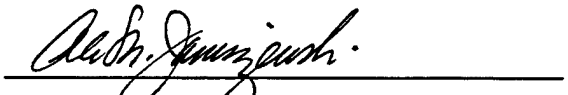

ALAN M. JANISZEWSKI, Lt Col, USAF
Chief
Power Division

Do not return copies of this report unless contractual obligations or notice on a specific document requires its return.

REPORT DOCUMENTATION PAGE

Form Approved
OMB No. 0704-0188

1. AGENCY USE ONLY *(Leave blank)*	2. REPORT DATE	3. REPORT TYPE AND DATES COVERED
	May 1998	Final Report, 06/01/95 - 06/01/97

4. TITLE AND SUBTITLE

Missile Fin Heat Pipe Cooling

5. FUNDING NUMBERS

PE JMP090
PR ARMP
TA 94
WU 00

6. AUTHOR(S)

Brian D. Donovan, Won S. Chang, Joseph M. Gottschlich

7. PERFORMING ORGANIZATION NAME(S) AND ADDRESS(ES)

Power Division
Air Force Research Laboratory
Wright Patterson AFB OH 45433-7251

8. PERFORMING ORGANIZATION REPORT NUMBER

9. SPONSORING/MONITORING AGENCY NAME(S) AND ADDRESS(ES)

PROPULSTION DIRECTORATE
AIR FORCE RESEARCH LABORATORY
AIR FORCE MATERIEL COMMAND
WrRIGHT-PATTERSON AFB OH 45433-7251
POC: Brian Donovan, AFRL/PRPG (937) 255-6241

10. SPONSORING/MONITORING AGENCY REPORT NUMBER

AFRL-PR-WP-TR-1998-2066

11. SUPPLEMENTARY NOTES

12a. DISTRIBUTION AVAILABILITY STATEMENT

Approved for public release distribution is unlimited.

12b. DISTRIBUTION CODE

13. ABSTRACT *(Maximum 200 words)*

The main objective of this project was to determine if heat pipe technology could be used to cool the portion of a missile's control surfaces heated by hot exhaust gas. The goal was to reduce the heat conducted into the body of the missile and its actuation rod. The small portion of the airfoil near the missile body heated by the exhaust plume is to be cooled by rejecting the heat to the large portion of the fin moving through ambient air. It is a ground-to-ground missile with a maximum speed of about Mach 0.75, but the evaporator will see exhaust gas (after shock) at mach 0.89 and 1213 K. The heat pipe was built inside a NACA 0015 airfoil of chord length 0.1143 m, the first 0.05 m of the fin will be heated by the exhaust plume. The report summarizes the aerodynamic heat and cooling approximations used, basic heat pipe theory, design specifications for the missile fin test article, transient heat pipe start-up calculations, experimental setup and testing of the proof-of-concept test article.

14. SUBJECT TERMS	15. NUMBER OF PAGES
Heat Pipe, Missile, Fin, Cooling, Liquid Metal	54
	16. PRICE CODE

17. SECURITY CLASSIFICATION OF REPORT	18. SECURITY CLASSIFICATION OF THIS PAGE	19. SECURITY CLASSIFICATION OF ABSTRACT	20. LIMITATION OF ABSTRACT
UNCLASSIFIED	UNCLASSIFIED	UNCLASSIFIED	SAR

Table of Contents

List of Figures

List of Tables

List of Symbols

A = cross-sectional area
A_v = heat pipe cross-sectional area
A_w = cross-sectional area of wick
C_1 = heat capacity per length (frozen)
C_2 = heat capacity per length (liquid)
C_p = specific heat per unit length
F = frictional coefficient
g = acceleration due to gravity
h_{fg} = latent heat of evaporation
h_{sl} = latent heat of fusion
K = wick permeability
l = characteristic length (vapor)
L = length
p = heat pipe perimeter
Q_c = capillary limit
Q_e = heat flux into the evaporator
Q_{ent} = entrainment limit
Q_f = heat flow to free molecular region
Q_s = sonic limit
R = gas constant of working fluid
r_c = effective capillary radius
$r_{h,s}$ = hydraulic radius
th = thickness
T_{hp} = heat pipe temperature
T_{melt} = melting temperature
T_t = transition temperature
T_∞ = ambient temperature
Z = continuum front location
Z_c = length of condenser
Z_e = length of evaporator
Δt = time step
Δt_{melt} = time to melt working substance
ε = porosity of the wick
γ = ratio of specific heats

μ = dynamic viscosity

ρ = density

σ = surface tension

Subscripts

c = condenser

e = evaporator

l = liquid (working fluid)

p = heat pipe container material

s = solid (working fluid)

v = vapor (working fluid)

w = wick

Acknowledgments

We thank Bill Nourse and Don Thomas of U.S. Army Missile Command for sponsoring this research activity and for providing technical information concerning the missile flight conditions and structure. Thanks are also due to Dick Harris for experimental setup and testing support.

1. Statement of the Problem

1.1 Background

The main objective of this project is to determine if heat pipe technology can be used to cool the portion of a missile's control surfaces heated by hot exhaust gas. The goal is to reduce the heat conducted into the body of the missile and its actuation rod. The small portion of the airfoil near the missile body heated by the exhaust plume is to be cooled by rejecting the heat to the large portion of the fin moving through ambient air. It is a ground-to-ground missile with a maximum speed of about Mach 0.75, but the evaporator will see exhaust gas (after shock) at Mach 0.89 and 1213 K. Figure 1 is a simplified illustration of the physical situation.

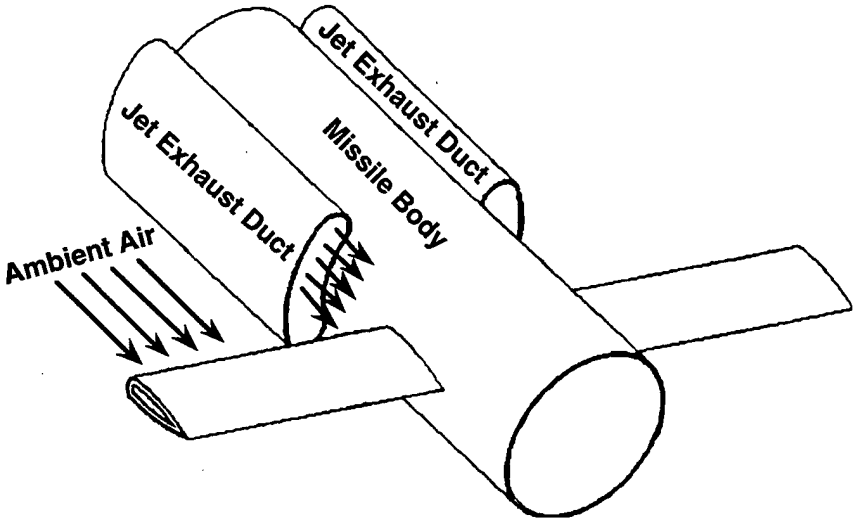

Figure 1. Simplified conceptual drawing of the missile configuration.

(Note: There are also two vertical fins, one above and one below the missile body)

The ambient air temperature is assumed to be 300 K, but since this missile could be deployed anywhere, temperatures as low as 240 K are possible during transport or even operation. Thus, a frozen startup scenario is possible for even room temperature working fluids.

1.2 Physical Requirements

The heat pipe is to be built inside a NACA 0015 airfoil of chord length 0.1143 m (see Figure 2). The total length of the heat pipe will only be a small portion of the 0.254 m span of the fin. The first 0.05 m of the fin will be heated by the exhaust plume. The heat pipe shell has to withstand a pressure difference of approximately 1.7 atmospheres during flight. The heat pipe will be subjected to a launch acceleration load of 2g along the launch flight path until a maximum speed of Mach 0.75 is reached This acceleration is expected to be short lived (~20 seconds). The bottom fin on the missile will be placed in an evaporator up configuration requiring the working fluid to wick up against gravity. Little maneuvering is anticipated until the final few seconds of flight. ***There must be an axial hole, 0.0159 m diameter, through the heat pipe for an actuation rod.*** Figure 3 illustrates how the heat pipe is an integral part of the fin.

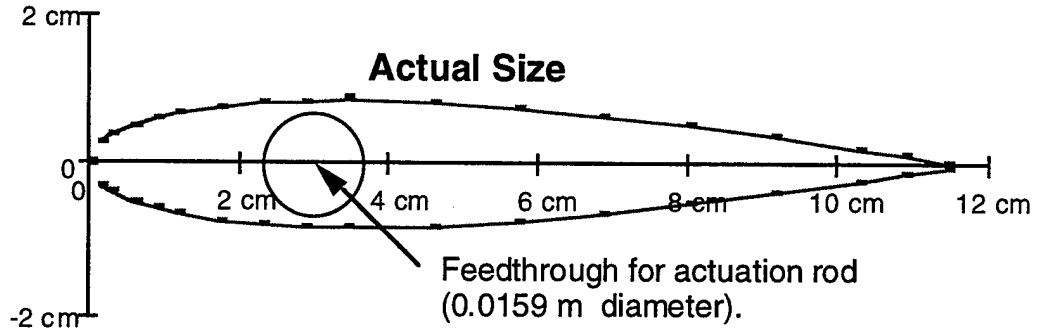

Figure 2. Heat pipe fin cross-section.

1.3 Aerodynamic Heating & Cooling Estimates

The phase 1 final report, by Chang (1995), included a method to estimate the heat transfer coefficient for the airfoil used in this project. Basically, the airfoil is treated as a flat plate except for the leading edge portion. This front part of the fin is treated as a circular cylinder because the flat plate correlation would greatly over estimate the convection heat transfer coefficient, h, for this portion of the fin. These estimated values have been used in order to facilitate temperature dependent h estimates for both the evaporator and condenser portions of the heat pipe for various operating temperatures.

1.3.1 Circular Cylinder Heat Transfer Coefficient

The main challenge is to find the appropriate diameter of the circular cylinder used for this estimate. Through graphical and computational analysis, a diameter of 0.0127 m was used for this estimate. This circular cylinder correlation is used for the first 0.007 m along the airfoil surface from the leading edge stagnation point. This translates to 63° of the cylinder. The average h for the leading edge is approximated by the following equation:

$$\bar{h}_{cyl} = h_\theta\Big|_{0^\circ}^{63^\circ} = 1.042\left(\frac{k}{D}\right)\left(\frac{\rho u D}{\mu}\right)^{0.5} Pr^{0.4}$$

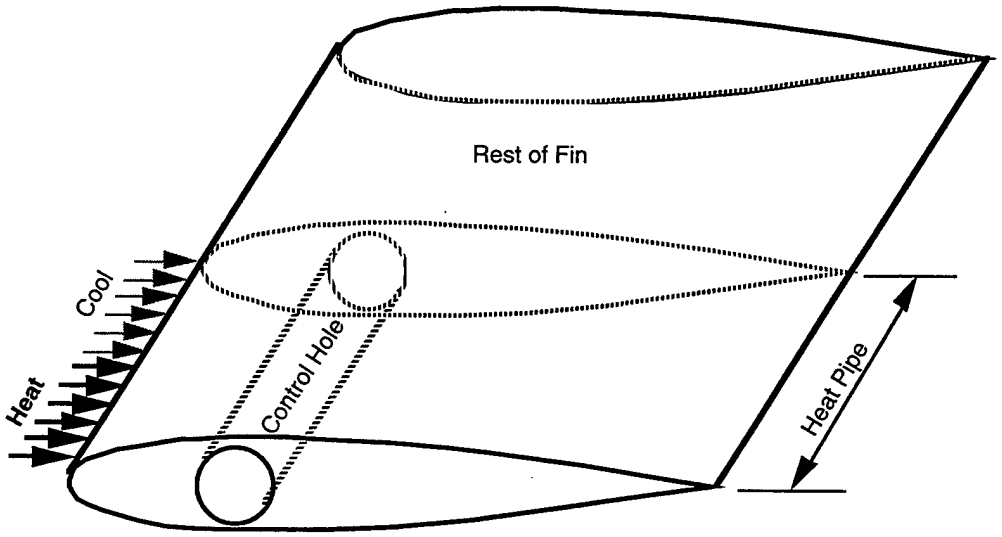

Figure 3. Simplified illustration of heat pipe fin.

1.3.2 Flat Plate Heat Transfer Coefficient

The remaining surface of the air foil, 0.007 m to 0.116 m, is assumed to be a flat plate. The average heat transfer coefficient, $\bar{h}$, for this region is estimated from

$$\bar{h}_{fp} = h_x\Big|_{0.007m}^{0.116m} = 0.0542(k)\left(\frac{\rho u}{\mu}\right)^{0.8} Pr^{1/3}$$

1.3.3 Combined Estimate of Heat Transfer Coefficient

In order to illustrate how well the 0.0127 m diameter circular cylinder correlation matches up to the flat plate correlation from x=0.007 m, Figure 4 shows h as a function of surface coordinate distance from the leading edge stagnation point for an evaporator temperature of 900 K .

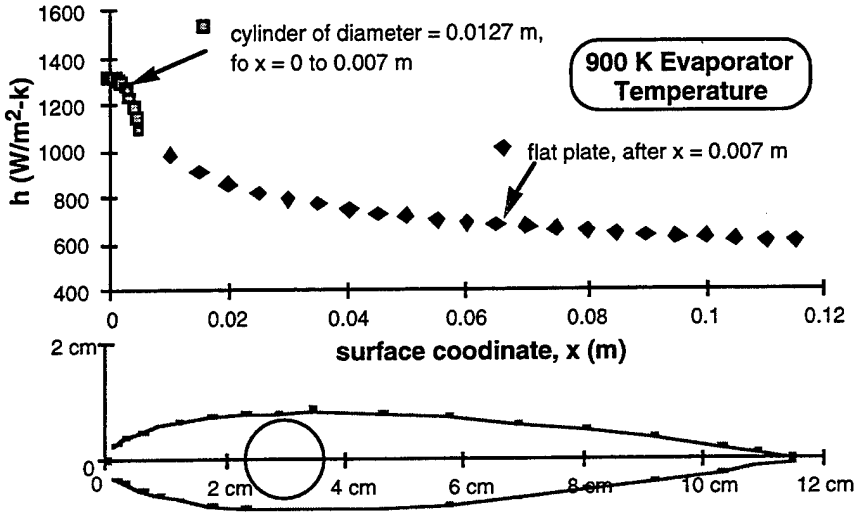

Figure 4. Heat transfer coefficient, h, profile for an evaporator temperature of 900 K.

The average convection heat transfer coefficient, $\bar{h}_{ave}$, is of course the weighted average of the $\bar{h}_{cyl}$ and $\bar{h}_{fp}$ given above.

$$\bar{h}_{ave} = \frac{0.007}{0.116}\bar{h}_{cyl} + \frac{0.109}{0.116}\bar{h}_{fp}$$

2. Heat Pipe Background

2.1 Theoretical Performance Limitations

There are many limitations on the operating capability of a heat pipe, but the major constraint is usually the capillary limit. The entrainment and sonic limits are sometimes relevant. Chang (1995) gave a good tutorial on these limits in the phase 1 report, and a detailed description can be found in Chi (1976).

2.1.1 Capillary Limit

$$Q_c = \frac{\frac{2\sigma}{r_c} - \rho_l g(L_e + L_c)}{\frac{(L_e + L_c)}{2}(F_l + F_v)}$$

where r_c is the effective capillary radius, ρ_l is the liquid density, g is the acceleration due to gravity, L_e and L_c are the evaporator and condenser lengths. F_l and F_v are frictional coefficients for the liquid and vapor sections:

$$F_l = \frac{\mu_l}{KA_w\rho_l h_{fg}}$$

$$F_v = \frac{(f_v Re_v)\mu_v}{2A_v r_v^2 \rho_v h_{fg}}$$

2.1.2 Sonic Limit

$$Q_s = A_v \rho_v h_{fg}\left[\frac{\gamma R T_v}{2(\gamma+1)}\right]^{1/2}$$

2.1.3 Entrainment Limit

$$Q_{ent} = A_v h_{fg}\left[\frac{\sigma\rho_v}{2r_{h,s}}\right]^{1/2}$$

2.2 Steady State Energy Balance

At steady state, the energy into the device must be the same as the energy taken out of the device. For this situation, the heat into the evaporator must be equal to the heat rejected at the condenser. The heat into the evaporator, Q, is given by

$$Q = pL_e h_e\left(T_{r,e} - T_e\right)$$

where p is the perimeter of the fin, h_e is the convection heat transfer coefficient for the evaporator, $T_{r,e}$ is the recovery temperature at the evaporator surface, and T_e is the outer wall temperature for the evaporator. A similar expression can be written for the condenser side and equated to the evaporator expression yielding

$$h_e A_e\left(T_{r,e} - T_e\right) = h_c A_c\left(T_c - T_{r,c}\right)$$

After dividing through by p, L_c can be resolved in terms of L_e:

$$L_c = L_e\left(\frac{h_e}{h_c}\right)\left(\frac{T_{r,e} - T_e}{T_c - T_{r,c}}\right)$$

The temperature drop across the fin wall and the saturated wick is calculated based on one-dimensional conduction of a steady state heat load, Q. The temperature of the inside wall of the heat pipe evaporator, $T_{w,e}$, is given by

$$T_{w,e} = T_e - \frac{Qt_p}{pL_e k_p}$$

where t_p is the wall thickness, and k_p is the thermal conductivity of the heat pipe container wall. Similarly, the vapor temperature, T_v, is calculated from

$$T_v = T_{w,e} - \frac{Qt_{wick}}{pL_e k_{eff}}$$

where t_{wick} is the wick thickness, and k_{eff} is the effective thermal conductivity of the saturated wick.

Unfortunately, the condenser temperature, T_c, is still an unknown in these equations. It can be determined by the following relationship:

$$T_c = T_v - \frac{Q}{pL_c}\left[\frac{t_{wick}}{k_{eff}} + \frac{t_p}{k_p}\right]$$

It can be easily seen that the above equations are coupled, but what is not obvious is that many of the equations have terms that are nonlinear functions of the temperatures (like the h's and k's). So this ends up to be a set of nonlinear coupled equations that must be solved in an iterative manner. Since it is desired that this heat pipe operates at as low a temperature as possible, solution of these equations is automated using a Microsoft Excel spreadsheet for several potential working fluids.

2.3 Operating Temperature .... Working Fluids

The desired operating temperature for this heat pipe is in the 600 - 700 K range. But from previous experience this seems improbable given the existing working fluids for this temperature range. The following sections outline the process of determining the best heat pipe working fluid for a given temperature range. This is done by estimating the heat transfer coefficient at the evaporator and condenser, then determining the total heat input to the evaporator, and then estimating the condenser length. These are all functions of temperature.

2.3.1 Average Heat Fluxes

The evaporator and condenser heat transfer coefficients have been approximated using flat plate and circular cylinder correlations. The leading edge of the air foil, from 0 to 0.007 m, is estimated to be a circular cylinder of 0.0127 m diameter; and the rear of the airfoil is approximated as a flat plate. The heat transfer coefficient, h, has a

maximum value at the leading edge and steadily decreases with the chord length (see Figure 4). The calculated average heat transfer coefficients are plotted in Figure 5.

Now given values for h as a function of evaporator and condenser temperatures, Q, q, and L_c can be calculated as functions of temperature. These quantities are important in determining a feasible working fluid and operating temperature.

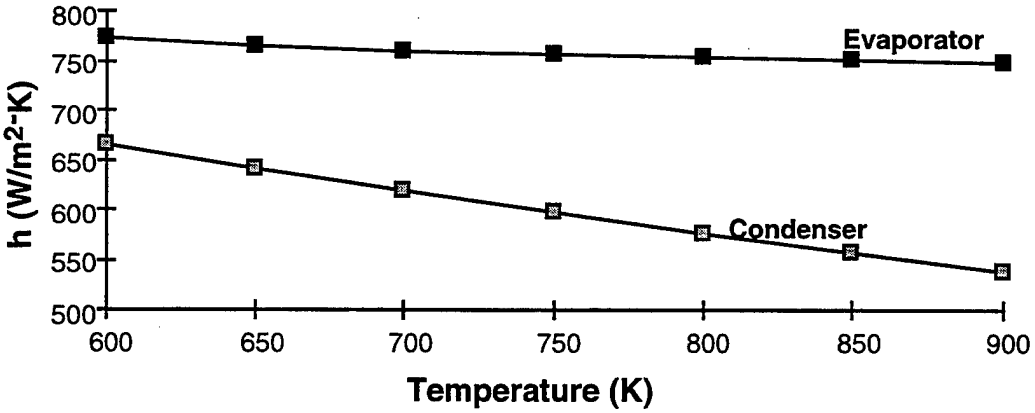

Figure 5. Calculated average heat transfer coefficients as a function of temperature for the evaporator and condenser.

The heat flux into the evaporator section of the heat pipe is a function of the heat pipe operating temperature. Using the estimates for h given above, the total heat input as a function of evaporator temperature has been calculated and is illustrated in Figure 6. As expected, the heat input to the evaporator decreases as the evaporator temperature increases.

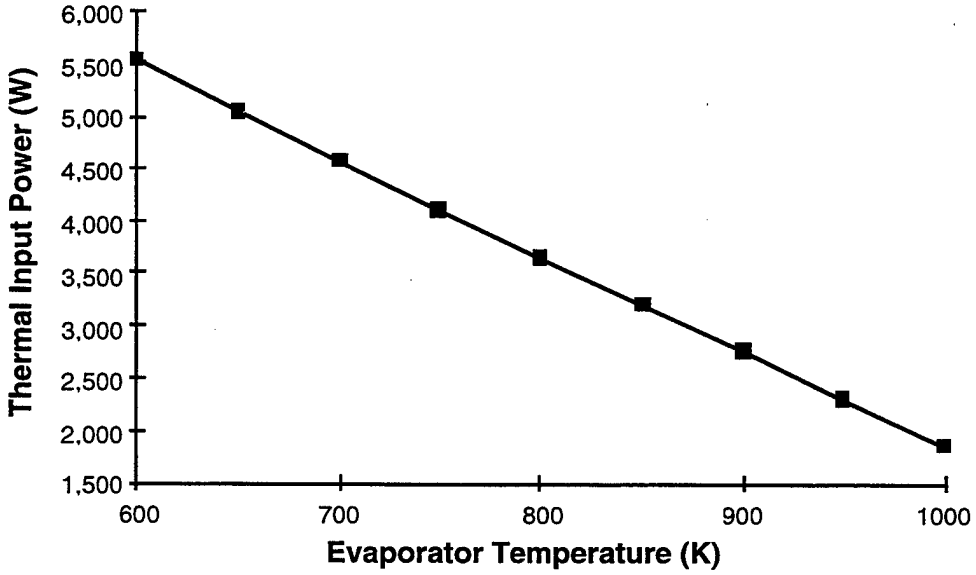

Figure 6. Thermal input power, Q, as a function of evaporator temperature.

2.3.2 Evaporator Average and Maximum Heat Fluxes

The average and maximum (leading edge) heat fluxes have been calculated and plotted as a function of evaporator temperature in Figure 7. As can be seen from Figure 7, the average heat fluxes are very high below 800 K and are likely to be beyond the capability of most known working fluids for that temperature range. The leading edge heat fluxes are typically about twice the average fluxes, making the situation even worse.

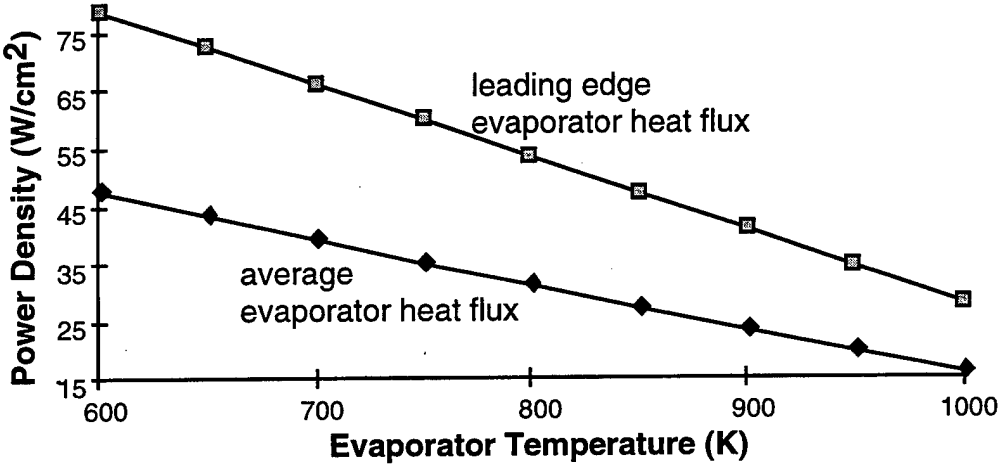

Figure 7. Leading edge and average heat fluxes into the evaporator as a function of evaporator temperature.

2.3.3 Condenser Length

Even if a working fluid can be found to operate in the desired temperature range and handle the heat fluxes, there may still be a practical limit on the length of the condenser given that this is a short fin. Condenser lengths for various evaporator temperatures have been calculated and plotted in Figure 8. It can be seen from this figure that at 600 K, the condenser length would be about 0.2 m. Given that the evaporator length is fixed at about 0.5 m, it may be feasible to operate at 600K if a suitable working fluid can be found.

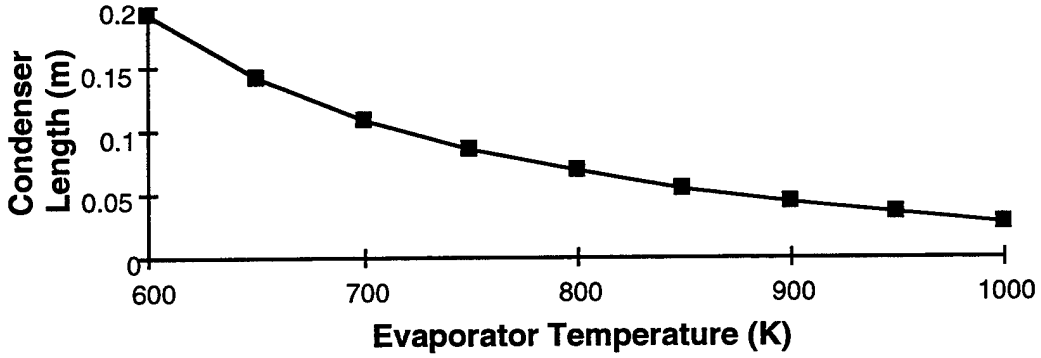

Figure 8. Calculated condenser lengths as a function of evaporator temperature.

2.3.4 Working Fluids

Now that it has been shown from an energy balance that the fin is long enough to accommodate a 600 - 700 K heat pipe, it must be determined if there is a working fluid that can do the job. Figure 9 shows most of the useful heat pipe working fluids and their useful operating temperature ranges. It can be seen from this figure that Hg, Cs, and H_2O are the only possibilities at 600 - 700 K.

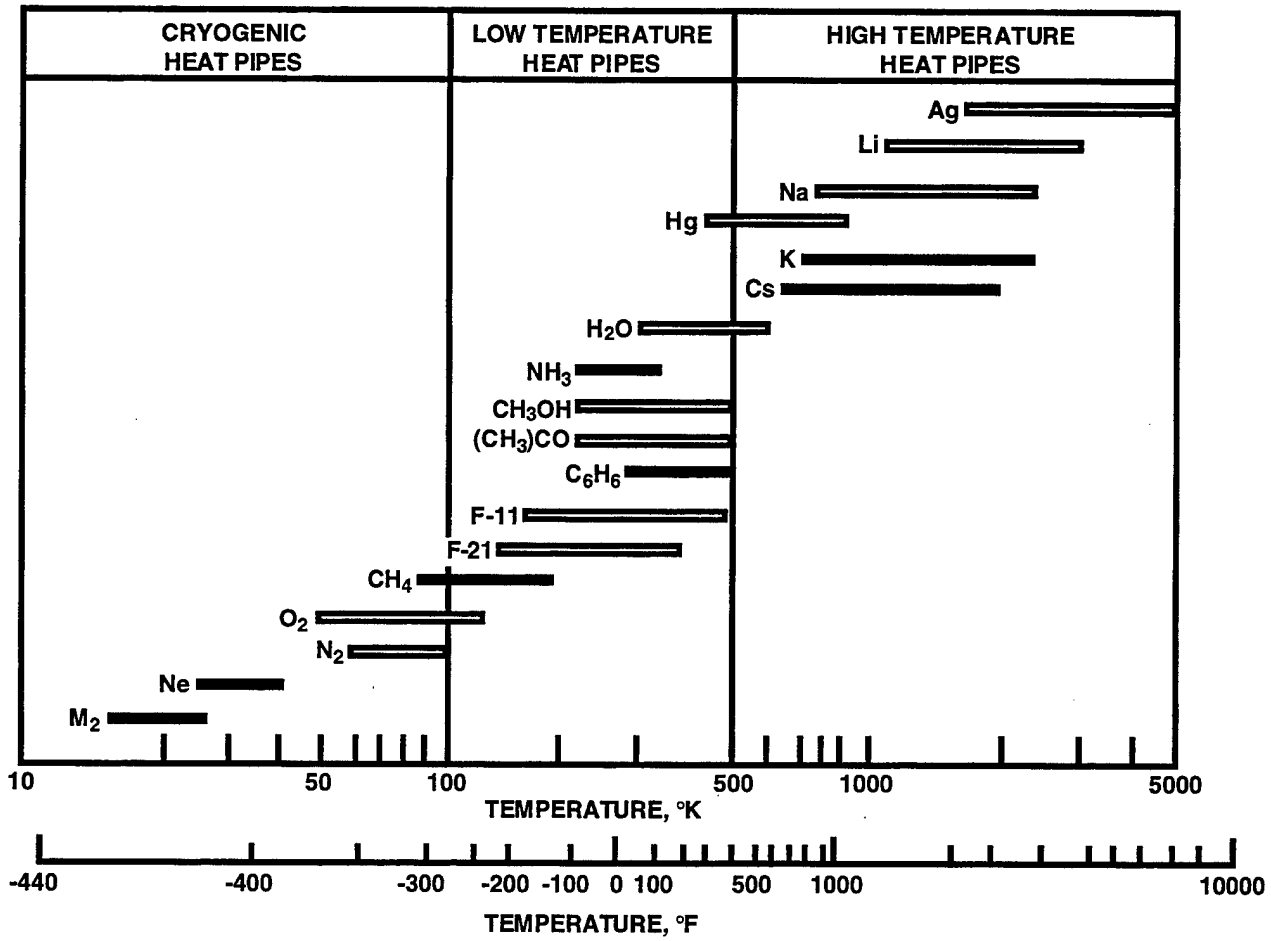

Figure 9. Heat pipe working fluids and operating temperatures (Chi, 1976).

Now, given that these three working fluids can operate in this temperature range, it must be determined if any of them can handle the required heat loads. One indicator of the heat transport capability of a fluid is the liquid transport factor, N_l, defined as the surface tension times the latent heat divided by kinematic viscosity:

$$N_l = \frac{\sigma\lambda}{\nu_l}$$

Figure 10 shows N_l as a function of temperature for water, Hg, and Cs. Water is clearly an unacceptable working fluid near or above 600 K. This fact is not surprising because water has a critical temperature of about 643 K. It can also be seen that Cs has a very low N_l in general, making it an unacceptable working fluid for this high heat flux application. It does appear that Hg has a N_l that could be acceptable.

The next indicator to look at is the wicking height factor, H. This factor is defined as the ratio between the surface tension and the density times gravitation acceleration. This term gives an indication of how great a pressure head can be supported in the wick of the heat pipe. This term is important for this application given that the working fluid must wick up against gravity in the bottom fin. This term is given by

$$H = \frac{\sigma}{\rho_l g}$$

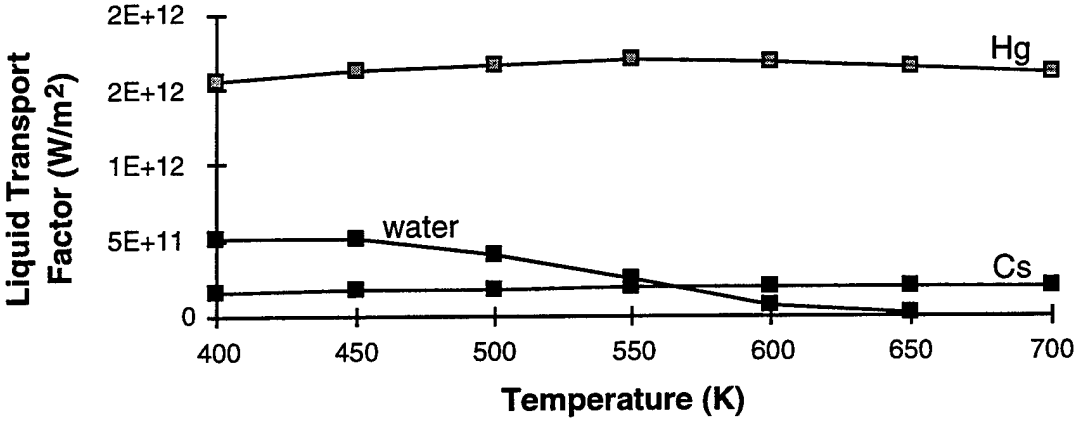

Figure 10. Liquid transport factors as a function of fluid temperature (Data from B & K Volume II).

Figure 11 plots H as a function of fluid temperature for water, Hg, and Cs. Again, it is clear from this figure that water is unacceptable anywhere near 600 K. Unfortunately, Cs and Hg also have poor values of H for the required wicking distance of this application.

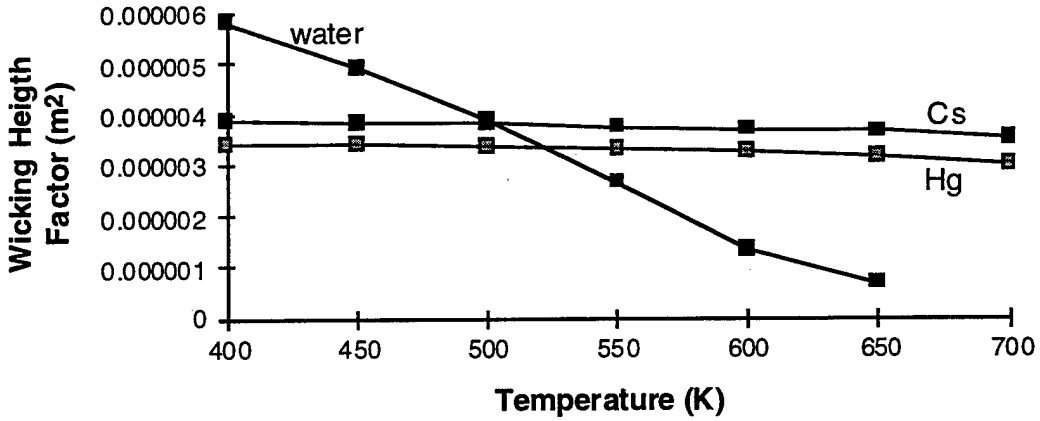

Figure 11. Wicking height factors as a function of fluid temperature (Data from B & K Volume II).

2.3.5 Selection of Working Fluid

From the above discussion, it may appear that Cs and Hg are not acceptable however, calculations must be done to be certain. The calculations were run for both working fluids, and they all are capillary limited at all temperatures calculated.

After these calculations were accomplished, there was only the remote possibility that one of Mainstream's new working fluids could do the job. Mainstream, a Florida based thermosciences company, was given the heat flux requirements and other pertinent physical requirements to evaluate if one of these new fluids would be suitable for this application. Mainstream estimates that none of these new fluids is close to having the required transport and wicking ability for this application.

This left no choice but to use either Na or K as the working fluid; and this fact imposes that the operating temperature must be above 800 K. At 900 K, Na has a N_l of 2.2×10^{12} W/m^2 and an H of 1.76×10^{-5} m^2, which should be adequate for this application.

3. Could Insulation Help?

Don Thomas of the US Army Missile Command raised an interesting question: If enough insulation were placed between the heat source and the heat pipe working fluid, could the heat pipe operate at a temperature suitable to use water as the working fluid? This is certainly an interesting question and worth exploring further.

To facilitate answering this question, consider the simplified model of this hypothetical conduction path illustrated in Figure 12. Accounted for here are the conduction paths for the stainless steel fin wall (k_{fin}, x_{fin}), insulator material (k_{ins}, x_{ins}), heat pipe wall (k_{hp}, x_{hp}), and heat pipe wick (k_{wick}, x_{wick}). Neglected are all of the contact resistances between the material layers. For a steady state situation, the heat flow (q) through each layer in Figure 12 will be the same:

$$q/A = \frac{k_{fin}}{x_{fin}}(T_s - T_1) = \frac{k_{ins}}{x_{ins}}(T_1 - T_2) = \frac{k_{hp}}{x_{hp}}(T_2 - T_3) = \frac{k_{wick}}{x_{wick}}(T_3 - T_v)$$

where T_s is the outer surface temperature of the fin, and T_v is the vapor temperature of the heat pipe as before. The intermediate temperatures can easily be eliminated:

$$q/A = \frac{(T_s - T_v)}{\frac{x_{fin}}{k_{fin}} + \frac{x_{ins}}{k_{ins}} + \frac{x_{hp}}{k_{hp}} + \frac{x_{wick}}{k_{wick}}} = \frac{(T_s - T_v)}{D}$$

The heat flux input is determined by the free stream temperature (T_∞) and the free stream convection coefficient (h_∞):

$$q/A = h_\infty(T_\infty - T_s) = \frac{(T_s - T_v)}{D}$$

This equation can now be solved for T_s:

$$T_s = \left(\frac{h_\infty D}{1 + h_\infty D}\right)T_\infty + \left(\frac{1}{1 + h_\infty D}\right)T_v$$

Now the fin surface temperature T_s can be easily solved as a function of insulator thickness, x_{ins}, if all other parameters are held constant. For this calculation, the vapor

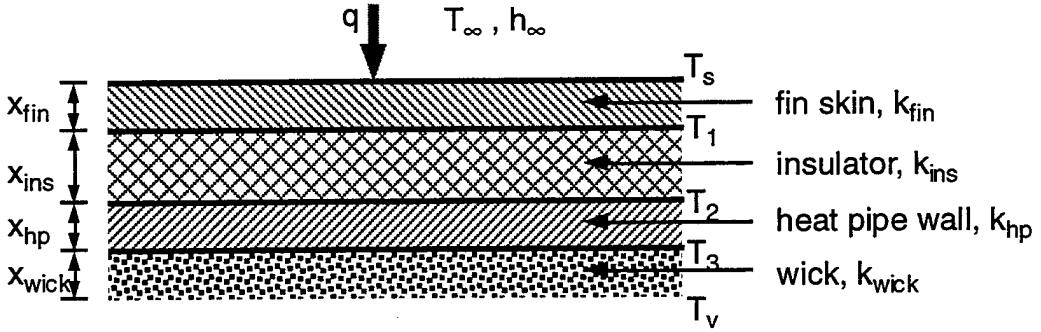

Figure 12. Simplified conduction path including an insulation layer.

temperature (T_v) will be fixed at 473 K, close to the upper practical operating limit for water. Values of 1200 W/m^2-K for h_∞ and 1213 K for T_∞ are used as in the previous heat pipe calculations. The other parameters used for this calculation are shown in Table 1.

Table 1. Parameters Used for Calculation.

	x (m)	k (W/m-K)	material
fin skin	0.0023	22	stainless steel
insulator	variable	0.058	Fiberfrax Ceramic Fiber Paper (HSA)
heat pipe wall	0.0023	375	copper
wick	0.00023	1.22	copper/water

Figure 13 shows both the fin skin temperature and the input heat flux to the evaporator as a function of the insulator thickness for a heat pipe vapor temperature fixed at 473 k. In this simplified calculation, the fin surface temperature increases rapidly as with increases in insulator thickness. As the fin skin temperature increases, the heat flux into fin rapidly decreases because this is driven by the temperature difference between the fin and the free stream temperature. There would of course be a practical upper limit to the fin skin temperature; and for stainless steel this would be around 1000 K. It can be seen in Figure 13 that the insulator thickness corresponding to a 1000 K fin temperature is just slightly above 0.0001 m, predicting a heat flux of

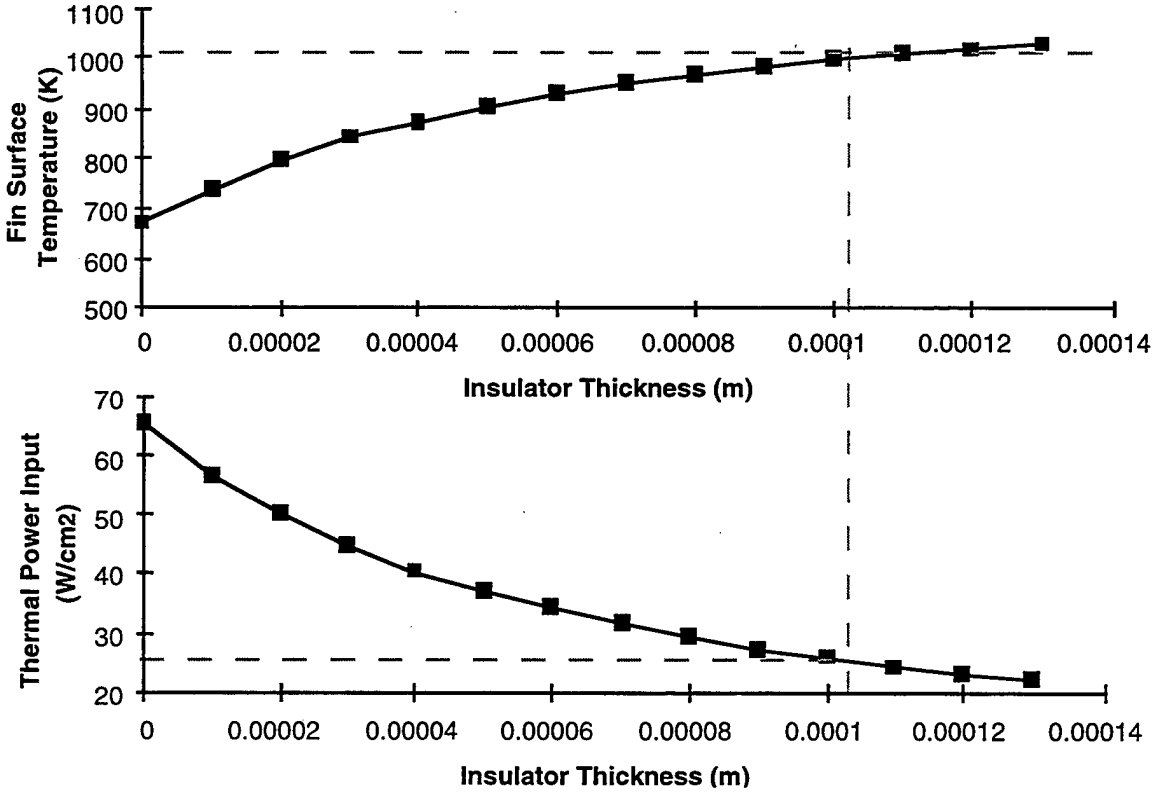

Figure 13. Fin skin temperature and thermal input heat flux as a function of insulator thickness.

about 25 W/cm^2.

These calculations are clearly based on assumptions that overly simplify the actual physical situation, but the results suggest that the use of a water heat pipe in this type of situation is feasible. A copper/water heat pipe is certainly feasible near 25 W/cm^2 or below, and the insulator thickness required to get this heat flux is only minimal. This idea certainly warrants further more thorough exploration.

4. Heat Pipe Design Specifications

Thermacore Inc., a small business in Lancaster PA specializing in heat pipe technology, was given the following specifications to fabricate a stainless steel - Na heat pipe to operate above 800 K with the thermal input and heat fluxes indicated in Figure 14. Table 2 contains relevant heat pipe parameters.

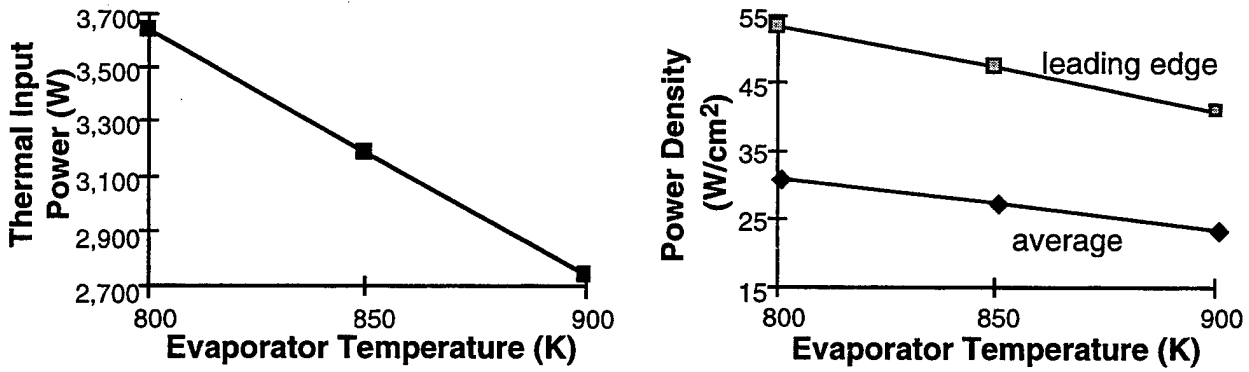

Figure 14. Heat flux and thermal input information.

Table 2. Heat Pipe - Fin Parameters

Item	Specification
Operating Temp	800 - 900 K
Wall Material	304 Stainless Steel (SS)
Working Fluid	Sodium (Na)
Wick	200 mesh 304 SS screen
Configuration Shape	NACA 0015 (c=0.1143 m)
Wall Thickness	0.0023 m
Evaporator Length	0.050 m
Condenser Length	0.055 m
Input Power	3,186 W @ Te = 850 K
Evaporator Heater	Radiant removable
Condenser Cooler	heat choked water
Total Fin Length	0.254 m
Acceleration Field	Short duration 3g

Thermacore built and delivered two proof-of-concept heat pipe fins. Appendix A contains a fabrication summery written by Thermacore, and Appendix B has the fabrication and assembly drawing that Thermacore used. Both heat pipes failed shortly after steady-state testing due to a faulty weld.

5. Transient Analysis

An analytical model similar to those developed by Silverstein (1971), Camarda (1977), and Chang (1996) was used to predict the transient operation from frozen start-up of a liquid metal heat pipe. The analytical model consists of lumped capacitance models representing the five possible physical stages encountered during the start-up of a liquid metal heat pipe from a frozen state. Figure 15 depicts the various stages of start-up described in detail below.

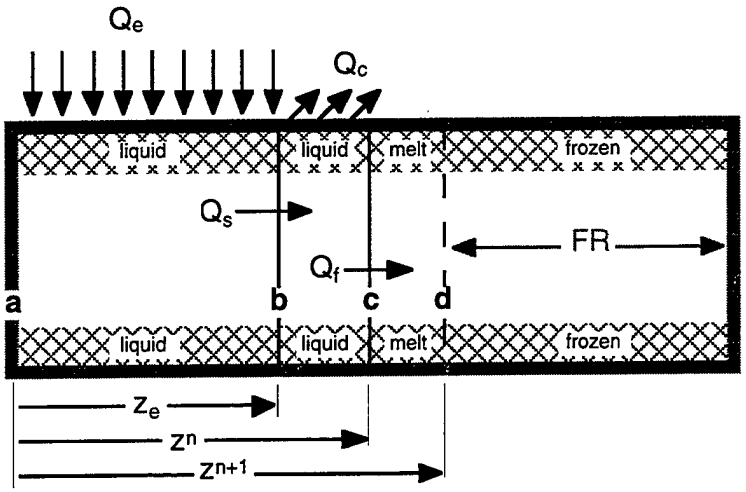

Figure 15. Control volumes used for transient analysis.

5.1 Stage 1: Frozen Working Substance

This stage predicts the transient temperature increase of the evaporator from heat input to the evaporator. The assumptions for this stage are: a) the evaporator can be treated as one lumped capacitance body; b) only the evaporator changes in temperature with heat input to the evaporator; c) the working substance remains in a frozen state during this stage. Therefore, for $T_{hp} < T_{melt}$, the new temperature of the heat pipe after a time step, Δt, is predicted by

$$T_{hp}^{n+1} = T_{hp}^{n} + \frac{Q_e \Delta t}{C_1 z_e} \qquad (1)$$

where $C_1 = (\rho C_p)_p A_p + (1-\varepsilon)(\rho C_p)_w A_w + \varepsilon(\rho C_p)_s A_w$.

5.2 Stage 2: Evaporator Thaw

This stage predicts the time required to thaw, Δt_{melt}, the working substance in the evaporator. The assumptions for this stage are: a) the evaporator can be treated as one lumped capacitance body; b) only the evaporator is heated; c) there is no change in temperature. Therefore, for $T_{hp} = T_{melt}$, the time to melt the evaporator section is given by

$$\Delta t_{melt} = \varepsilon \rho_l A_w z_e \frac{h_{sl}}{Q_e} \qquad (2)$$

5.3 Stage 3: Evaporator Heating to Transition Temperature

This stage predicts the transient temperature increase of the thawed evaporator up to the transition temperature, T_t, of the working fluid, predicted by

$$T_t = 4990\frac{\pi}{R}\left(\frac{\mu_v}{\rho_v l}\right)^2 \qquad (3)$$

Due to the temperature-dependent properties of the parameters used in equation (3), the transition temperature must be calculated using an iterative process. The assumptions for this stage are: a) the evaporator can be treated as one lumped capacitance body; b) only the evaporator changes in temperature with heat input to the evaporator; c) the vapor space is a free molecular region, thus heat transport out of control volume a-b in Figure 15 is neglected. Therefore, for $T_{melt} < T_{hp} < T_t$, the new temperature of the heat pipe after a time step, Δt, is predicted by

$$T_{hp}^{n+1} = T_{hp}^{n} + \frac{Q_e \Delta t}{C_2 z_e} \qquad (4)$$

where $C_2 = (\rho C_p)_p A_p + (1-\varepsilon)(\rho C_p)_w A_w + \varepsilon(\rho C_p)_l A_w$.

5.4 Stage 4: Melt Front Propagation

In this stage, heat pipe operation begins as the continuum front moves down the length of the heat pipe. The assumptions for this stage are: a) the continuum region, length z^n, can be treated as one lumped capacitance body; b) the continuum region is established initially over the entire evaporator region, z_e, as soon as the transition temperature is reached; c) $T_t < T_{hp}$ and $z_e < z^n < z_e + z_c$. An energy balance of control volume b-c in Fig. 15 gives

$$Q_f = Q_s - h_c p\left(z^n - z_e\right)\left(T_{hp}^n - T_\infty\right) - \frac{C_2\left(z^n - z_e\right)}{\Delta t}\left(T_{hp}^{n+1} - T_{hp}^n\right) \qquad (5)$$

Similarly, an energy balance of control volume a-c gives

$$Q_e = Q_f + h_c p\left(z^n - z_e\right)\left(T_{hp}^n - T_\infty\right) + \frac{C_2 z^n}{\Delta t}\left(T_{hp}^{n+1} - T_{hp}^n\right) \qquad (6)$$

Finally, an energy balance on control volume c-d in gives the next continuum front position after time step, Δt, given by

$$z^{n+1} = z^n + \frac{\Delta t Q_f}{C_1\left(T_{melt} - T_\infty\right) + C_2\left(T^{n+1} - T_{melt}\right) + \rho\varepsilon A_w h_{sl}} \qquad (7)$$

Equations (5) and (6) are coupled and nonlinear due to temperature-dependent properties, so an iterative solution process must be used to solve for Q_f and T^{n+1} using the current continuum front position, z^n. Equation (7) is then solved once Q_f and T^{n+1} have been determined. This stage is continued until the continuum front reaches a steady-state position, or the continuum front reaches the end of the condenser (stage 5).

5. Stage 5: Condenser-Limited Heat Pipe Operation

In this stage, the entire heat pipe is active and the transient temperature increase is predicted until steady-state temperature is reached. The assumptions for this stage are: a) the entire heat pipe can be treated as one lumped capacitance body; b) the continuum region is established over the entire heat pipe length, $z^n = z_e + z_c$. The new temperature of the heat pipe after a time step, Δt, is predicted by

$$T_{hp}^{n+1} = T_{hp}^{n} + \frac{(Q_e - Q_c)\Delta t}{C_2(z_e + z_c)} \qquad (8)$$

5.6 Startup Predictions

The procedures and stages for predicting the transient startup of a liquid metal heat pipe outlined in equations (1) - (8) were implemented using a Mathematica 2.2 program. A program listing and sample calculation is provided in Appendix C. Mathematica was chosen to implement this model due to its built-in iteration capabilities and solvers for systems of coupled (even non-linear) equations.

Figure 16 is the transient prediction for the front heat pipe. The top portion of the figure is a prediction of the evaporator temperature until the transition temperature

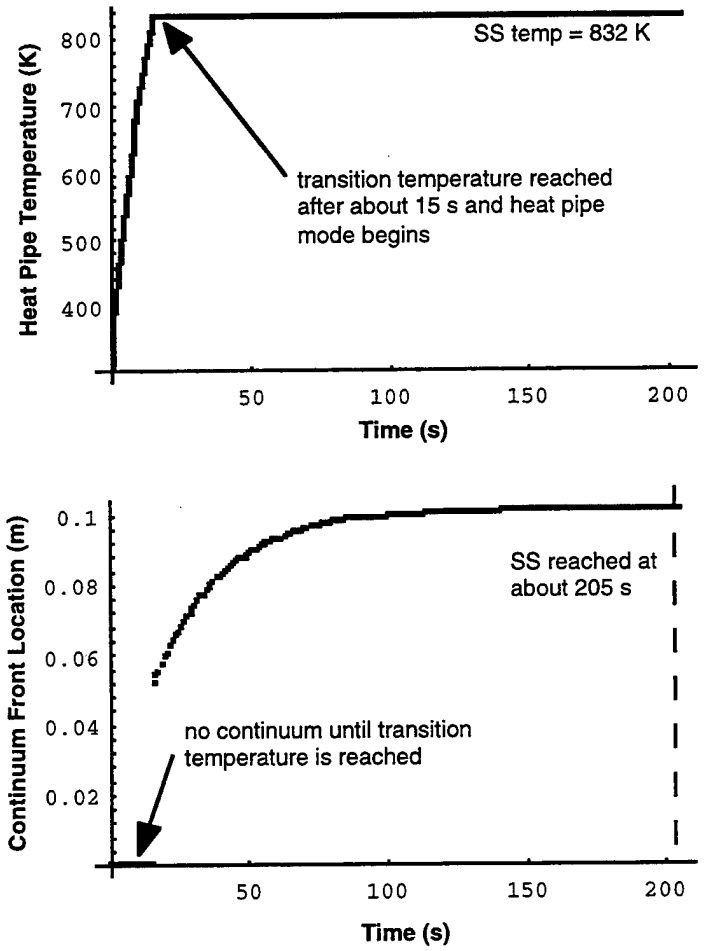

Figure 16. Transient prediction for front pipe.

(832 K) is reached, then it is the temperature of the continuum region. As shown here, the model has assumed that the heat pipe will operate at the transition temperature unless the condenser length is too short. The bottom portion of Figure 16 is the predicted continuum front propagation after start up. It can be seen here that there should be no continuum front until the transition temperature is reached, then the front begins to propagate past the evaporator section. The steady-state time predicted to be 205 seconds by determining where this curve reaches its asymptotic maximum. Note that since this curve does appear horizontal at steady-state, the condenser length is long enough. If the condenser length is too short, the continuum front verses time curve would stop short of horizontal as the end of the condenser is reached, and the temperature would increase above the transition temperature.

A similar prediction can be seen in Figure 17 for the rear heat pipe. The rear heat pipe is predicted to reach a steady state operating temperature of 822 K after 212 seconds.

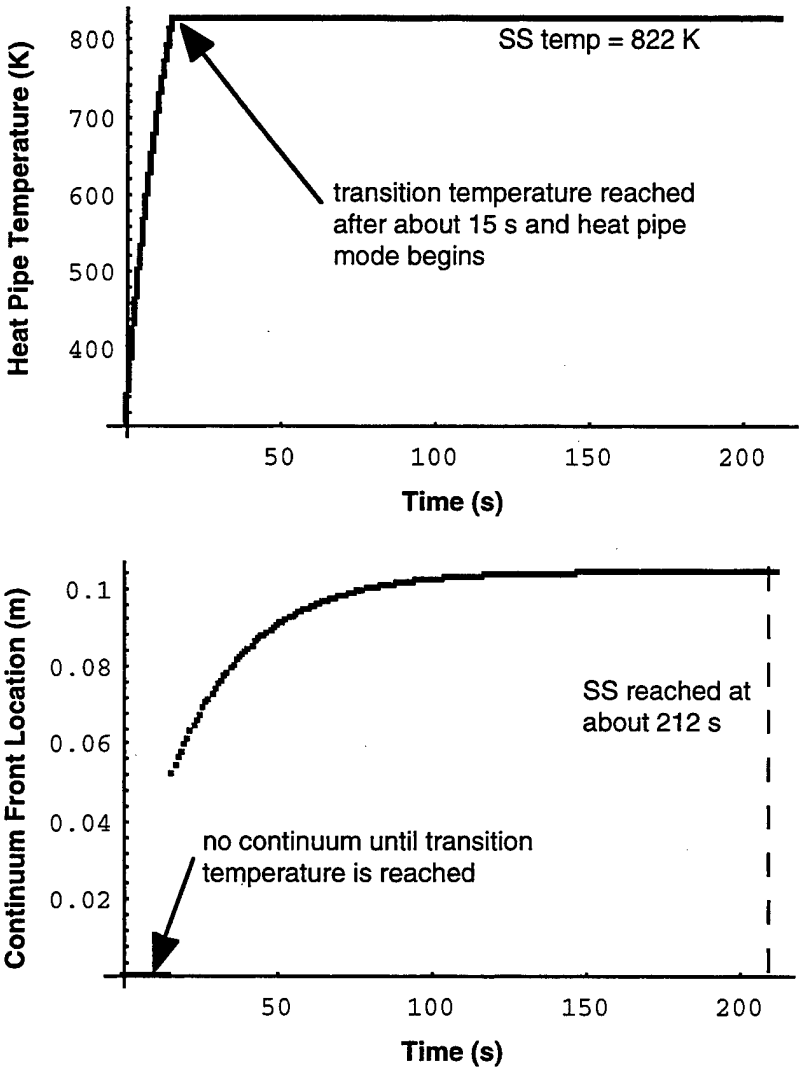

Figure 17. Transient prediction for rear pipe.

6. Results and Conclusions

Two proof-of-concept heat pipe fins, one shown in Figure 18, were fabricated by Thermacore and verified for steady-state operation. Appendix A contains a fabrication summery written by Thermacore, and Appendix B has the fabrication and assembly drawings that Thermacore used. Both heat pipes failed shortly after steady-state testing due to a faulty weld. As a result, the transient predictions cannot be validated and the use of a liquid metal heat pipe for this transient-in-nature application cannot be fully proven. It should be noted that this failure was due to a fabrication problem and not a design problem.

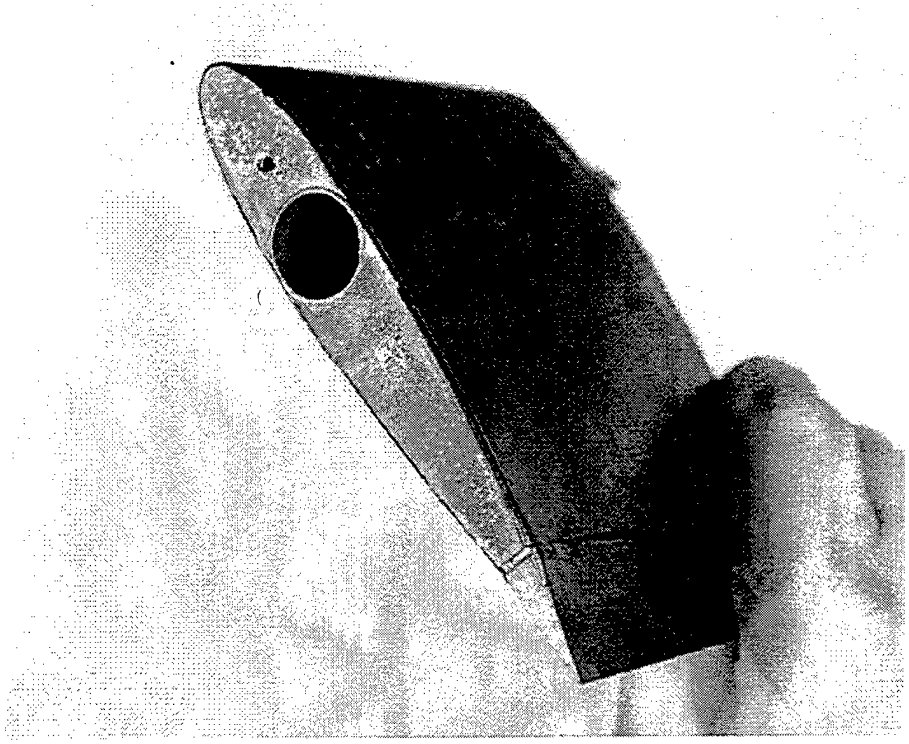

Figure 18. Proof-of-concept heat pipe fin.

6.1 Steady-State Results

The experimental results of the steady state testing are given in detail in Appendix A, but some of the more pertinent observations follow:

Table 3. Experimental steady-state results.

Case	Predicted SS Temp (K)	Actual Front HP Temp (K)	Actual Rear HP Temp (K)
1	820	839	854
2	820	852	881
3	820	820	831
4	820	819	829
5	820	832	829
6	820	793	825
average	**820**	**825.83**	**841.5**

It can readily be seen from Table 3 that the predicted steady-state temperature is within 1% of the average experimental value for the vapor space thermocouple on the front heat pipe, and within 3% of the average vapor space value for the rear heat pipe.

7. Cost Summary

The following is a breakdown of how the funds received by MIPR from the Army Missile Command were used:

Labor hours	$43K
Heat Pipe Fabrication	$39K
Test equipment	$ 8K

	$90K

8. References

Brennan, P. J. and Kroliczeck, E. J., 1979, "Heat Pipe Design Handbook," Volumes I & II, B & K Engineering, Inc., NTIS, N81-70112 and N81-70113.

Camarda, C. J., 1977, "Analysis and Radiant Heating Tests of a Heat-Pipe-Controlled Leading Edge," NASA TN-8486.

Chang, W. S., 1995, "Cooling Feasibility of a Missile Fin Exposed to Hot Exhaust Gas Using Liquid-Metal Heat Pipes," Final Report to the U.S. Army Missile Command.

Chang, W. S., 1996, "Startup of the Liquid-Metal Heat Pipe in Aerodynamic Heating Environments," WL-TR-96-2039, Wright-Patterson AFB, OH.

Chi, S. W., 1976, Heat Pipe Theory and Practice. A Sourcebook , Hemisphere Publishing Corporation, Washington, DC.

Silverstein, C. C., 1971, "A Feasibility Study of Heat-Pipe-Cooled Leading Edges for Hypersonic Cruise Aircraft," NASA CR-1857.

Appendix A:

Thermacore Fabrication Summary

THERMACORE

INC

Contract F33601-96-C-0009

MISSILE FIN HEAT PIPE

FINAL REPORT

February 5, 1997

Prepared for:

Wright Laboratory
Wright-Patterson Air Force Base, Ohio 45433

A DTX COMPANY

3.0 TECHNICAL APPROACH

This section of the report describes the technical approach used to meet the heat pipe fin specifications listed in the solicitation, as summarized in Appendix A. Each specification is addressed in the following discussion.

1. Operating temperature between 800K and 900K.

Thermacore has completed a preliminary analysis of the missile fin heat pipe, based on the information given in Appendix A. Due to the size of the control hole, the fin was divided into two separately operating heat pipes: one in front of the control hole and one behind the control hole. A calculation was made to estimate the sonic limit for the front heat pipe, which will be subjected to the larger axial heat flux. It was found that the front heat pipe must rise to a temperature of about 900K for conservative operation of the front heat pipe below the sonic limit to occur. Thus, operation of this device under simulated operating heating conditions probably will not allow normal operation of the front heat pipe at 800K, although the required test conditions will be at lower leading edge heat fluxes than actual operating heat fluxes, so this limit may not be observed in testing.

2. Wall material.

Thermacore assembled the missile fin proof-of-concept device from 0.090" thick 304L stainless steel sheet, joined primarily by welding. Sodium heat pipes using welded formed sheet construction were designed and built by Thermacore under Air Force Contract F33615-86-C-3227, as described below under References and Proof of Performance.

3. Working fluid.

Sodium was the selected working fluid. It has been successfully used in several leading edge heat pipes previously built by Thermacore. In addition to the work described in Item 2 above, Thermacore's large solar receiver heat pipe program is based on sodium heat pipe technology.

4. Wick Material.

A porous metal nickel (-50 + 100) wick structure rather than a stainless steel screen wick was selected for this application. Thermacore has had good success with this type of wick structure for our Solar Applications products, i.e. sodium/superalloy heat pipe solar receivers. Contracts listed in the reference list provide several examples. Absorbed heat fluxes of up to 100W/cm^2 are regularly achieved with sodium working fluid using such wicks. In addition, sintered porous wicks with a distribution of pores have been analytically and experimentally shown to be boiling tolerant, in contrast to single pore size wicks such as layered screens. This approach will thus provide a favorable performance margin for the missile fin application. Preliminary analysis has shown that a twofold safety margin can be realized using this design. Wick properties for the recommended wick structure are summarized below.

permeability	=	3.5 E-11 m^2
pore radius	=	4.0 E-5 m
thermal conductivity	=	60 W/m/K
wick thickness	=	1.25 mm

5. Configuration shape NACA 0015 (c=0.1143 m).

Thermacore formed the configuration shape using techniques previously used successfully for related leading edge, turboshaft engine, and solar receiver geometries. The leading edge radius was shaped around a forming mandrel. The remainder of the fin shape was set by joining the cover sheet to machined end plates and internal stiffeners which were machined to the specifications listed in Appendix A of the solicitation. Thermacore also has an active program that uses the same approach for forming turboshaft engine vane heat pipes which have a similar shape to those required for the missile fin. This work is being done on US Army Contract DAAJ02-94-C0023, and also uses the same forming technologies proposed for use on the subject proposed work.

Instrumentation for testing the heat pipe included thermocouples to measure the vapor temperature of each heat pipe and to perform calorimetry on the test article. An instrumentation and assembly drawing was prepared and submitted to Wright Laboratory for review and approval prior to fabrication of the hardware.

6. Wall thickness 0.0023 m.

The device was formed from sheet 0.0023 m (0.090")in thickness, as described in Item 2 above.

7. Evaporator length 0.050 m.

Sizing calculations were performed using this evaporator length, which showed that the recommended approach will successfully handle the heat flux, power levels, and operating temperatures specified herein.

8. Condenser length 0.072 m.

The same analysis described in Item 7 above showed that the front heat pipe and possibly the rear heat pipe will require a condenser length longer than 5.5 cm to function as a normal heat pipe at prescribed conditions and convect heat from the condenser surfaces. Lengths of the heat pipe condensers were specified from detailed analyses performed during the final design, as shown in Appendix C.

9. Input power 3.186 kW at 850K.

Preliminary analysis showed that the selected design can handle the required input power. A radiant heat source was used, which is capable of supplying the required input power, as described under Item 10.

10. Evaporator heat radiant removable type.

Thermacore used quartz lamp heaters for testing the heat pipes. Thermacore has developed considerable experience using this approach for the solar receiver heat pipe programs described below under related work. A procedure for operating and testing the heat pipe was supplied with the hardware at the time of delivery.

11. Condenser cooler affixed heat choked water-cooled type.

Thermacore built and delivered a water-cooled clamp-on type condenser/calorimeter which was supplied with the heat pipe at time of delivery. Standoffs were used on the condenser so that the water

in the condenser does not boil and so that the heat pipe is able to operate normally without freezing the working fluid or "shocking" the heat pipe. This latter non-operational condition occurs when the condenser design is too efficient, and prevents the heat pipe condenser from operating at subsonic conditions during startup. Previous experience in design, fabrication, and testing of similar devices was used to produce a condenser capable of allowing the heat pipe to operate in conditions simulating normal operation.

12. Total fin length 0.254 m.

The total fin length and geometry was built based on the specifications listed in Appendix A, as attached. Sheet metal extensions were added to the heat pipes to form the full length of the fin.

13. Acceleration field 3g for short duration.

A preliminary analysis was performed which showed that, during the 20 second acceleration at 2g, the temperature rise of the heat pipe will not be enough to raise the heat pipe to operating temperature. Thus, acceleration effects on the heat pipe should be minimal except during the final seconds of flight. The latter condition also occurs over such a short time duration that, based on preliminary calculations, the heat pipe will not be adversely affected. These analyses are provided in Appendix C.

14. Evaporator location along portion of fin adjacent to missile body.

The recommended heat pipe design is based on this specification.

4.0 DESIGN AND FABRICATION OF THE MISSILE FIN HEAT PIPES

Thermacore completed a series of performance calculations to verify the specifications supplied by the Air Force and to size the heat pipe wick structure. Table 1 summarizes the as-built heat pipe specifications; the supporting calculations used to develop this design are given in Appendix C. Figure 4 shows the assembly drawing developed from the selected design. The design consists of two separate heat pipe vapor chambers. One heat pipe is located in front of the control hole; the second

TABLE 1. - Missile Fin Heat Pipe Design Specifications

Item	Specification
Operating Temperature	800 - 900 K
Wall material	304 Stainless Steel (SS)
Working Fluid	Sodium (Na)
Wick	-50 +100 Sintered powder nickel
Configuration Shape	NACA 0015 (c=0.1143 m)
Wall Thickness	0.0023 m
Evaporator Length	0.050 m
Condenser Length	0.072 m
Input Power	3,186 W @ Te = 850 K
Evaporator Heater	Radiant removable
Condenser Cooler	Heat choked water
Total Fin Length	0.254 m
Acceleration Field	Short duration 3g
Evaporator Location	Innermost edge of fin

heat pipe is located behind the control hole. Each heat pipe is lined with a 0.040" (1mm) thick layer of -50 +100 sintered nickel powder that serves as a heat pipe wick structure. The evaporator section of each heat pipe is located adjacent to the missile fin body; the heat absorbed by the heat pipe from the exhaust plume is spread along the heat pipe and rejected to air by convection and radiation. A welded extension is attached to the far end of the fin which is not a heat pipe, but is simply part of the control fin. The fill tube ends of the heat pipes protrude into the hollow inside of the extension.

A fabrication procedure was developed to assemble the heat pipe missile fin. Figure 5 lists the main assembly steps used in the procedure. Each heat pipe was assembled with several stainless steel tubes inserted into their vapor spaces to assist in testing. Each heat pipe in each of two fin test articles

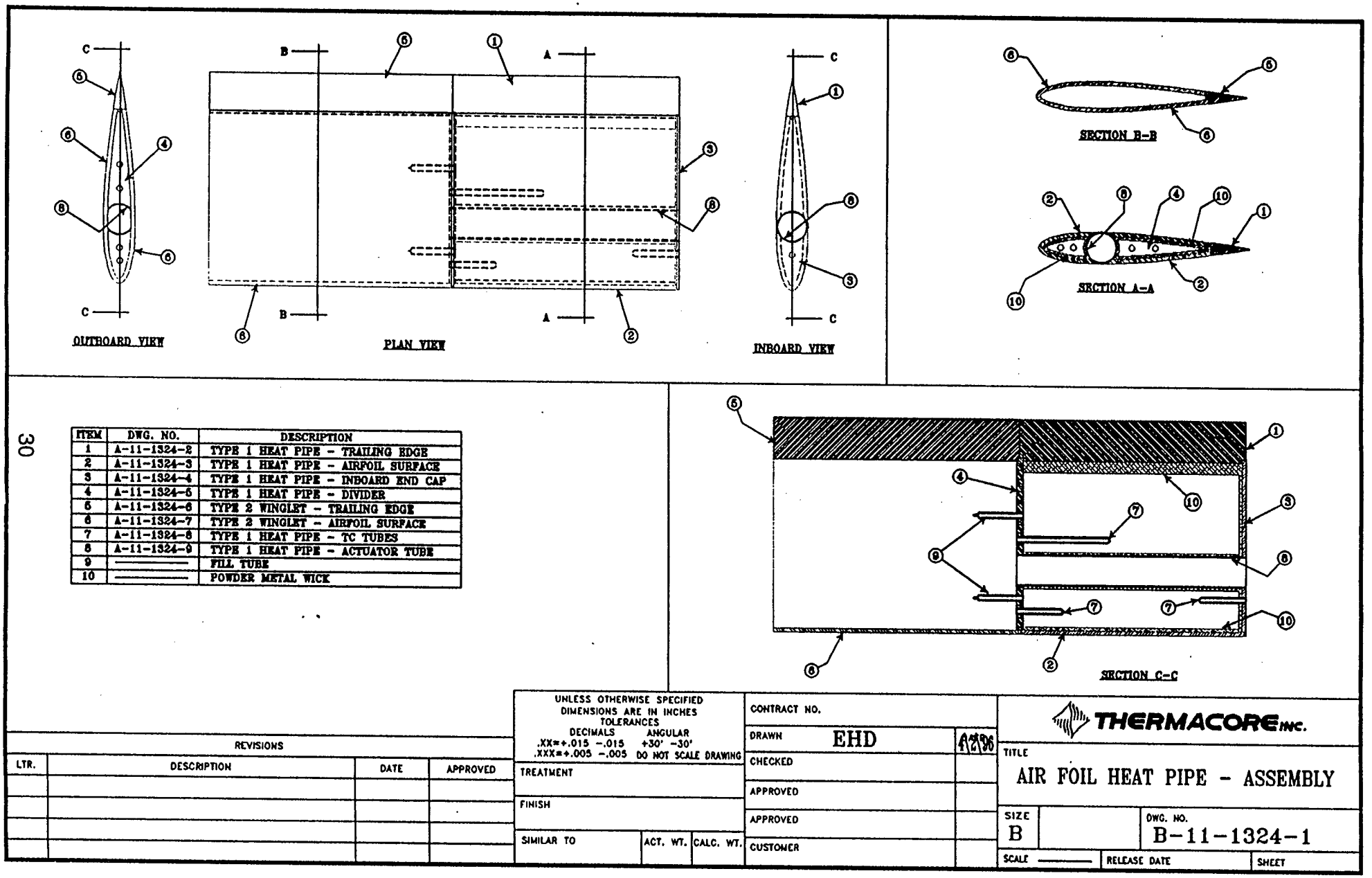

ITEM	DWG. NO.	DESCRIPTION
1	A-11-1324-2	TYPE 1 HEAT PIPE - TRAILING EDGE
2	A-11-1324-3	TYPE 1 HEAT PIPE - AIRFOIL SURFACE
3	A-11-1324-4	TYPE 1 HEAT PIPE - INBOARD END CAP
4	A-11-1324-5	TYPE 1 HEAT PIPE - DIVIDER
5	A-11-1324-6	TYPE 2 WINGLET - TRAILING EDGE
6	A-11-1324-7	TYPE 2 WINGLET - AIRFOIL SURFACE
7	A-11-1324-8	TYPE 1 HEAT PIPE - TC TUBES
8	A-11-1324-9	TYPE 1 HEAT PIPE - ACTUATOR TUBE
9	———	FILL TUBE
10	———	POWDER METAL WICK

REVISIONS			
LTR.	DESCRIPTION	DATE	APPROVED

UNLESS OTHERWISE SPECIFIED
DIMENSIONS ARE IN INCHES
TOLERANCES
DECIMALS ANGULAR
.XX=+.015 -.015 +30' -30'
.XXX=+.005 -.005 DO NOT SCALE DRAWING

TREATMENT

FINISH

SIMILAR TO | ACT. WT. | CALC. WT.

CONTRACT NO.

DRAWN EHD 4/26/96

CHECKED

APPROVED

APPROVED

CUSTOMER

THERMACORE INC.

TITLE
AIR FOIL HEAT PIPE - ASSEMBLY

SIZE B | DWG. NO. B-11-1324-1

SCALE ——— | RELEASE DATE | SHEET

Figure 4. Air Foil Heat Pipe - Assembly

was processed with sodium working fluid, and operated at temperatures of up to 800°C to vent any non-condensible gas that may be present from processing. All heat pipes operated successfully during these preliminary tests. Figure 6 shows two views of the assembled heat pipes, and illustrates the tack-welded screen pieces used to attach some of the thermocouples to the outer surfaces of the heat pipes. The remaining thermocouples were attached by sliding them into the tube inserts installed into the end caps of the heat pipes.

5.0 HEAT PIPE TESTING

Each test article was operated at temperatures up to 600°C using a pair of radiant quartz lamps for a heat source and a pair of clamped water calorimeters for a heat sink. Two views of the test setup are shown in Figure 7. Figure 8 shows data collected for each heat pipe during the first operating thermal cycle from cold startup, including a diagram showing the thermocouple locations.

During the first thermal cycle after the hot processing step, each heat pipe developed a similar failure in the form of a wall leak in the evaporator endcap next to the control hole. The failure manifested itself as a non-condensible gas leak into the front heat pipe, which revealed itself as a cold end in the condenser. The leak point was determined after cooldown to room temperature by visual inspection of the test articles; an alkali metal oxide spot formed on the surface of the fin at the leak locations. The first heat pipe was operated at power levels up to 1025 watts; the second heat pipe was operated at power levels of up to 297 watts.

The reason for the failure is believed to be caused by a combination of improper wall material, design specifications, and fabrication procedures. All previous thin-walled sodium heat pipe wing leading edges that were successfully developed by Thermacore used superalloys rather than 304 stainless steel for the envelope material, and all hardware used a minimum wall thickness of at least 0.035". This hardware includes the Boeing wing leading edges and the test articles built for Wright Laboratory on the cited SBIR program. Stainless steel is less favorable for applications where vacuum leaktight thin walls are required, since it is more susceptible to crystal grain growth and grain cracking than are superalloys. Furthermore, some of the procedures used to assemble the heat pipes could be modified

FABRICATION PROCEDURE FOR MISSILE FIN

1. CLEAN ALL PARTS IN ACETONE.
2. INSERT CENTERLESS GROUND TUBE IT SHELL AND TACK WELD END PLATES.
3. BRAZE TUBE WITH NICROBRAZE 30 AT 115O oC FOR 5 MINUTES
4. STOP-OFF WELD JOINTS.
5. INSPECT BRAZE JOINT REBRAZE IF NECESSARY.
6. WELD THERMOCOUPLE WELLS AND LEAK CHECK.
7. WELD THERMOCOUPLE WELLS TO END PLATES.
8. FABRICATE SOCK MANDRELS WITH 100 MESH 304 SS SREEEN.
9. TACK WELD EVAPORATOR END PLATE TO AIR FOIL.
10. INSERT SOCK MANDRELS.
11. FILL WITH -50 +100 NICKEL POWDER AND VIBRATE POWDER.
12. DRY HYDROGEN SINTER AT 1100 oC FOR 2 HOURS.
13. ELECTRON BEAM WELD END PLATES AND TAIL SECTION AND LEAK CHECK.
14. BRAZE CALORIMETER WITH NICROBRAZE LM.
15. VACUUM FIRE MISSILE FIN FOR 1 HOUR AT 900 oC.
16. CHARGE HEAT PIPES WITH SODIUM.
17. PROCESS HEAT PIPES AT SAME TIME.
18. SEND HEAT PIPE TO ELECTRON BEAM WELDER TO HAVE NON-HEAT PIPE FOIL WELDED TO HEAT PIPE.
19. SETUP LAMPS AND CALORIMETER FOR THERMAL TEST.
20. ATTACH THERMOCOUPLES TO THE HEAT PIPE.
21. TEST HEAT PIPE ON LAMPS WITH GAS-GAP CALORIMETER.
    1. Turn on water to lamps (2 GPM)
    2. Turn on air to lamps (17 CFM)
    3. Turn on water to calorimeter (250 cc's)
    4. Turn on controller to 1.1 on 10 turn pot, let lamps start, let heat pipe warm up. Let stabilize and turn power supply up in 0.1 increments,
    5. Let heat pipe temperature stabilize before turning up power supply.
1. TAKE PHOTOGRAPHS.

Figure 5. Fabrication Procedure for Missile Fin

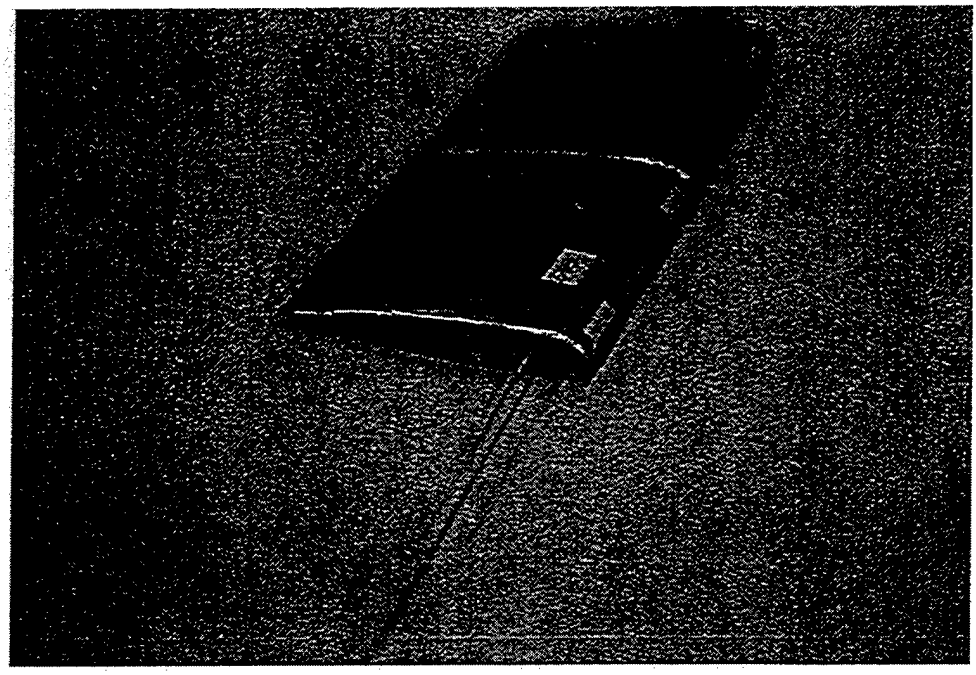

Figure 6a. Instrumented Missile Fin Test Article: View A

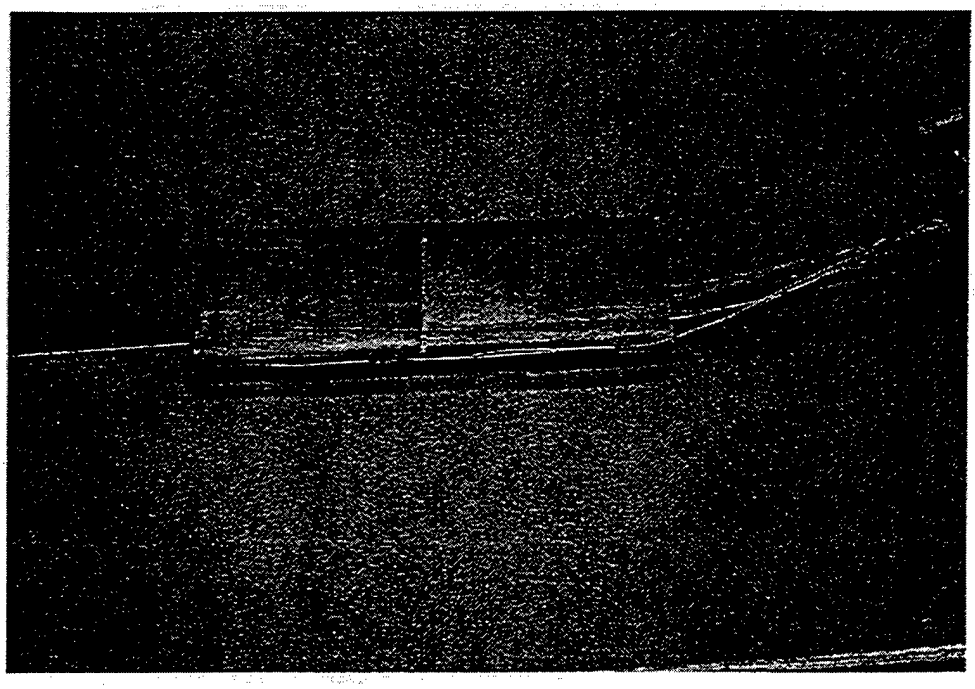

Figure 6b. Instrumented Missile Fin Test Article: View B

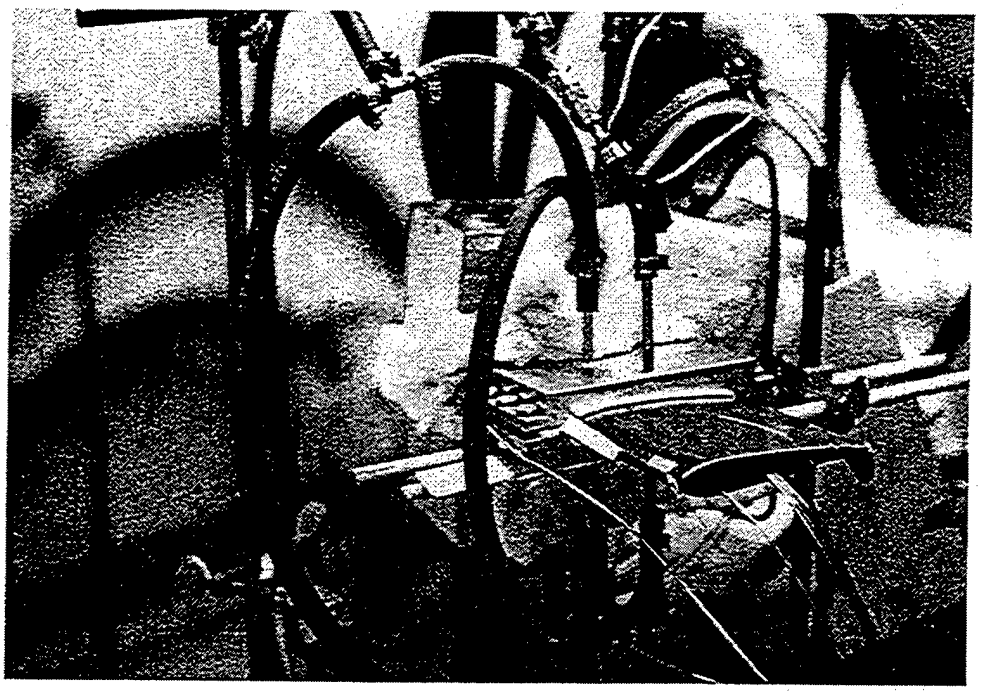

Figure 7a. Missile Fin Heat Pipe Test Setup: View A

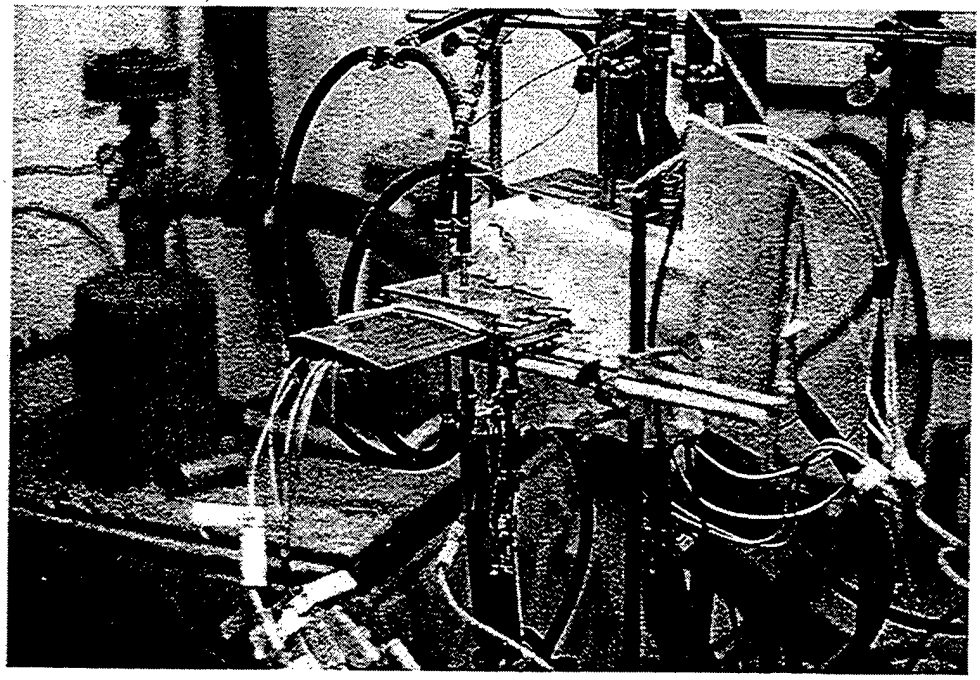

Figure 7b. Missile Fin Heat Pipe Test Setup: View B

DATE		Oct. 1,96	Oct. 1,96	Oct. 3,96	Oct. 3,96	Oct.8,96	Oct.8,96	Oct.9,96	Oct.10,96	Oct.11,96
TC No.	Location	Temp. C	Temp. C	Temp. C	Temp. C	Temp. C	Temp. C	Temp. C	Temp. C	Temp. C
1	Vap.LE	566	579	547	546	559	520	636	345	485
2	Cond.LE	304	344	380	370	307	295	504	154	175
3	Cond. RHP	581	608	558	556	556	552	549	213	226
4	Evap tube top	583	584	504	503	588	581		388	537
5	Evap tube side	636	607	517	615	650	652	#2HP	112	570
6	Evap tube bot	596	596	578	574	586	584		551	653
7	Evap tube side	628	602	612	610	658	661		503	624
8	Mid tube top	470	513	516	510	501	495		242	274
9	Mid tube side	473	510	506	495	469	460		211	260
10	Mid tube bot	573	584	555	549	546	541		288	294
11	Mid tube side	518	547	520	516	503	497		273	200
12	Cond tube top	328	366	383	375	311	302		184	160
13	Cond tube side	392	419	428	411	353	346		166	152
14	Cond tube bot	500	523	495	491	485	479		152	162
15	Cond tube side	466	494	470	466	432	426		172	160
16	Evap LE	574	569	573	572	591	593		332	400
17	Cond LE	289	331	383	371	322	311		166	156
18	Evap Top LE	636	698	639	636	701	711		723	727
19	Evap Bot. RHP	578	570	567	565	590	590		296	414
20	Water In	25	26.2	24.2	24.5	24.4	23.4		23.4	22
21	Water out	58.5	59.5	36	35.6	52.3	49.4		35	38.7
	Flow cc/min	254	254	800	908	500	563		254	254
	POWER	596	592	661	706	976	1025		206	297

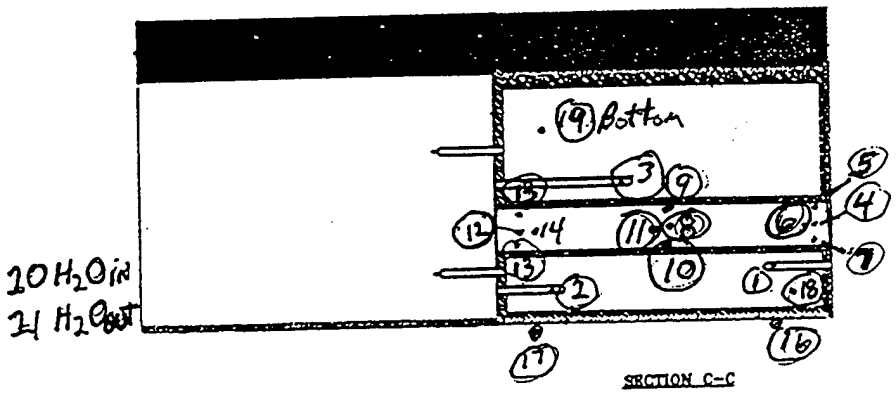

Figure 8.

to increase the likelihood of a design that would be resistant to thermal fatigue. The control hole tube/ envelope assembly was formed by brazing together two stainless steel pieces with wall thickness as small as 0.012"; joining was accomplished by brazing with Nicrobraze 30. Embrittlement of grain boundaries in the braze region certainly was a factor in the wall failures. Thermacore constructed heat pipes using wall thickness of 0.012" or thinner twice in the past. One design used a laminated hot isostatically pressed design composed of alternating layers of titanium foil and a mixture of titanium and titanium diboride powder (Rosenfeld et al., 1995) in a potassium heat pipe; the other design used a tungsten tube in a lithium heat pipe (Rosenfeld, 1992). Both of these approaches have been demonstrated successfully. It is believed that forming the missile fin envelope/control hole assembly from a single electric discharge machined (EDMed) plate would be a better fabrication approach because this would provide a single wall 0.024" thick with no embrittling braze material present in the wall. Welding rather than brazing is recommended for joining the end plates to the cover plates. Also, the use of oxygen getters is recommended to assist in suppressing wall grain boundary failures.

The heat pipes, quartz lamps, power supplies, and calorimeters were delivered to Wright Laboratory for further testing. This test report is being supplied to document the test results and design work, to assist the Air Force in defining future work in this area.

6.0 CONCLUSIONS AND RECOMMENDATIONS

Two stainless steel / sodium heat pipe missile fins were designed, built, and tested. Each heat pipe operated successfully during processing, but each fin failed in a similar manner during subsequent testing. Cause of failure was observed to be a failure of the front heat pipe envelope wall in the location near the control hole, where the wall thickness is only 0.024".

It is believed that by modifying several design parameters and fabrication steps, it is feasible to construct reliably operating heat pipe missile fins for this application. A summary of these recommended changes follows. Thermacore recommends fabrication of additional missile fins using the following changes.

1. Replace the stainless steel envelope material with Haynes 230 superalloy. This material has been demonstrated in several sodium heat applications at Thermacore under the solar dish Stirling heat pipe development program. It demonstrates superior weldability, oxidation resistance, fatigue resistance, grain growth resistance, and sodium compatibility.

2. Construct the missile fin assembly from a single block of metal by EDM, rather than by brazing together thin-walled subassemblies. This approach will provide a monolithic wall with small, crack-resistant metal grains. This approach will also allow construction of a completely welded missile fin assembly; brazing increases the likelihood of wall embrittlement for thin-walled assemblies in the braze region.

3. Use a piece of oxygen getter material such a hafnium, zirconium, or titanium in each heat pipe. This approach will reduce the likelihood of oxygen attacking grain boundaries and crevices inside the heat pipes.

7.0 REFERENCES

1. Chang, W. S., "Cooling Feasibility of a Missile Fin Exposed to Hot Exhaust Gas Using Liquid-Metal Heat Pipes," Final Report to the U.S. Army Missile Command, April 1995.

2. Donovan, Brian D., Joseph M. Gottschlich, and Won S. Chang, "Missile Fin Heat Pipe Cooling," Interim Report prepared for U.S. Army Missile Command, August 1995.

3. Rosenfeld, John H., "Porous Media Heat Exchangers for High Heat Flux Applications," SPIE Vol. 1739: High Heat Flux Engineering, pp. 41-50, 1992.

4. Rosenfeld, John H., William G. Anderson, Kevin Horner-Richardson, Robert F. Keller, and James T. Beals, "Space Power Thermal Management Materials and Fabrication Technologies for Commercial Use," AIP Conf. Proc. 324, pp.893-902, 1995.

5. Singh, Bhim S. and John H. Rosenfeld, "Directed Energy Thermal Shields," Final Report, Contract F33615-86-C-3227, 10 May 1989.

Appendix B:

Fabrication Drawings

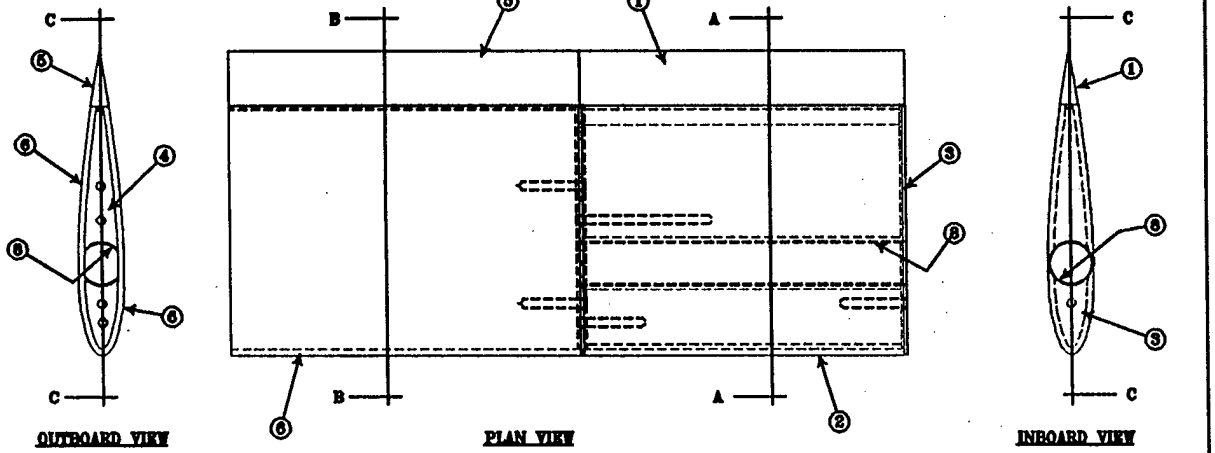

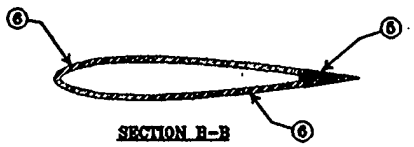
SECTION B-B

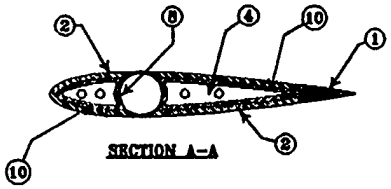
SECTION A-A

ITEM	DWG. NO.	DESCRIPTION
1	A-11-1324-2	TYPE 1 HEAT PIPE - TRAILING EDGE
2	A-11-1324-3	TYPE 1 HEAT PIPE - AIRFOIL SURFACE
3	A-11-1324-4	TYPE 1 HEAT PIPE - INBOARD END CAP
4	A-11-1324-5	TYPE 1 HEAT PIPE - DIVIDER
5	A-11-1324-6	TYPE 2 WINGLET - TRAILING EDGE
6	A-11-1324-7	TYPE 2 WINGLET - AIRFOIL SURFACE
7	A-11-1324-8	TYPE 1 HEAT PIPE - TC TUBES
8	A-11-1324-9	TYPE 1 HEAT PIPE - ACTUATOR TUBE
9	————	FILL TUBE
10	————	POWDER METAL WICK

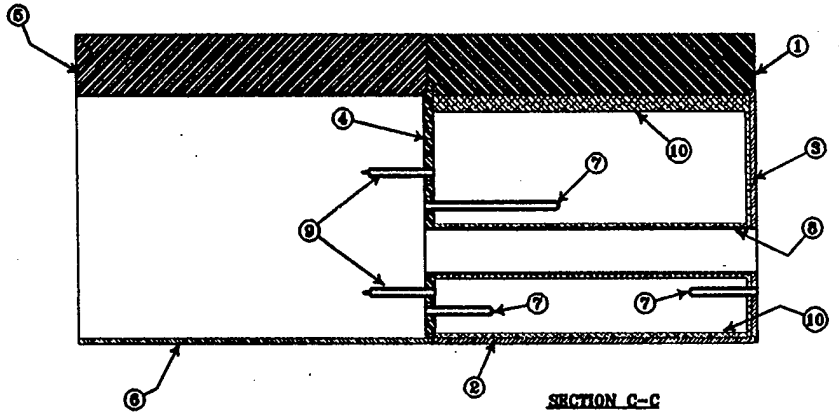
SECTION C-C

REVISIONS			
LTR.	DESCRIPTION	DATE	APPROVED

UNLESS OTHERWISE SPECIFIED
DIMENSIONS ARE IN INCHES
TOLERANCES
DECIMALS ANGULAR
.XX=+.015 -.015 +30' -30'
.XXX=+.005 -.005 DO NOT SCALE DRAWING

TREATMENT

FINISH

SIMILAR TO | ACT. WT. | CALC. WT.

CONTRACT NO.

DRAWN EHD 4/6/90

CHECKED

APPROVED

APPROVED

CUSTOMER

THERMACORE INC.

TITLE
AIR FOIL HEAT PIPE - ASSEMBLY

SIZE B | DWG. NO. B-11-1324-1

SCALE ———— | RELEASE DATE | SHEET

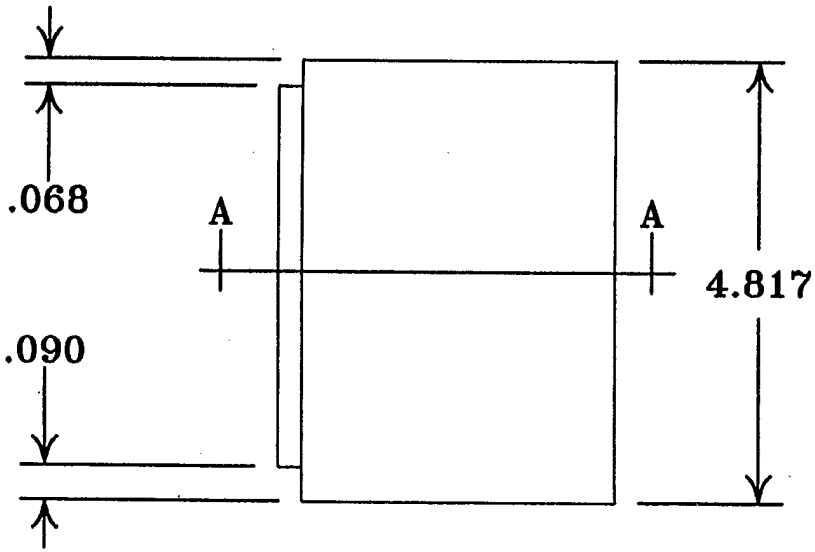

PT.	X	Y
1	−.125	.028
2	−.250	.049
3	−.375	.069
4	−.500	.089
5	−.625	.107
6	−.750	.126

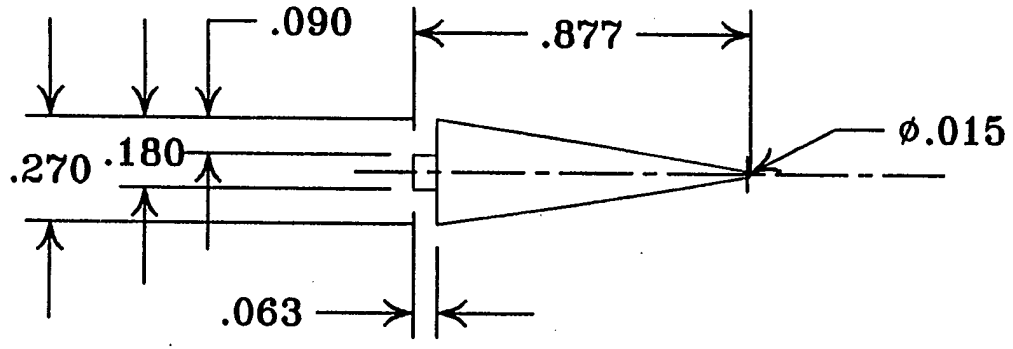

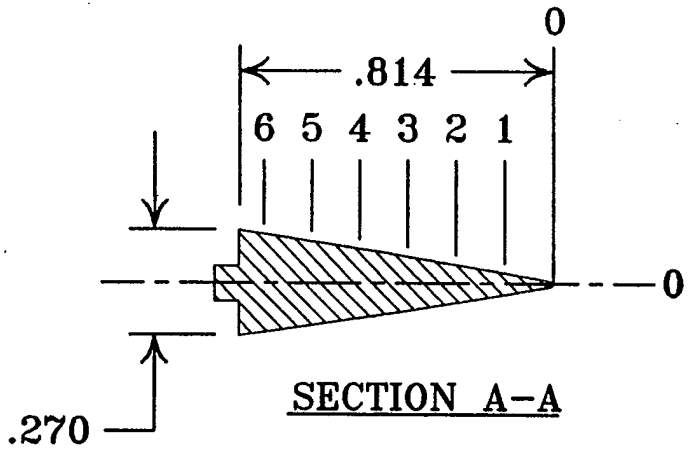

SECTION A-A

MATERIAL: 304 S.S.

UNLESS OTHERWISE SPECIFIED DIMENSIONS ARE IN INCHES TOLERANCES DECIMALS ANGULAR .XX=+.015 −.015 +30' −30' .XXX=+.005 −.005 DO NOT SCALE DRAWING	CONTRACT NO.		THERMACORE INC.
TREATMENT	DRAWN EHD	3\25\96	TITLE TYPE 1 HEAT PIPE-TRAILING EDGE
FINISH	CHECKED		
SIMILAR TO / ACT. WT. / CALC. WT.	APPROVED J L Lanzi	4\11\96	SIZE A / DWG. NO. A-11-1324-2
	APPROVED		SCALE — / RELEASE DATE / SHEET
	CUSTOMER		

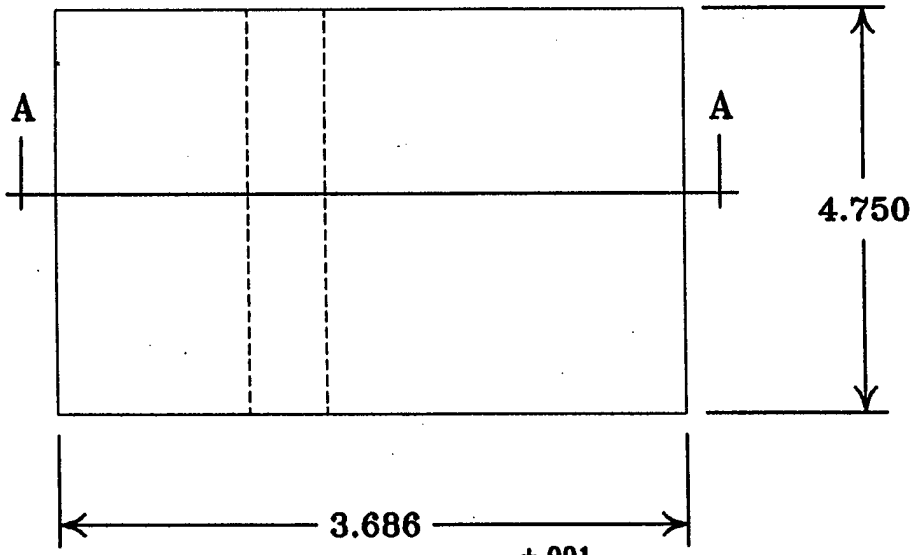

PT.	X	Y
1	.0563	.1065
2	.1125	.1471
3	.225	.1999
4	.3375	.2363
5	.45	.2634
6	.675	.3007
7	.9	.3227
8	1.125	.3342
9	1.35	.3376
10	1.8	.3264
11	2.25	.2978
12	2.7	.2567
13	3.15	.2061
14	3.6	.1476

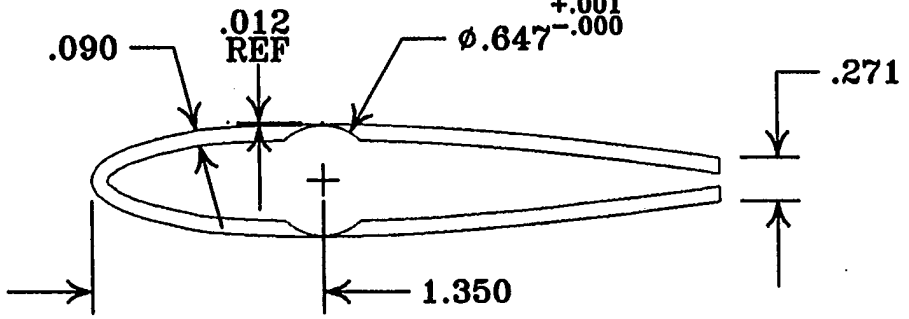

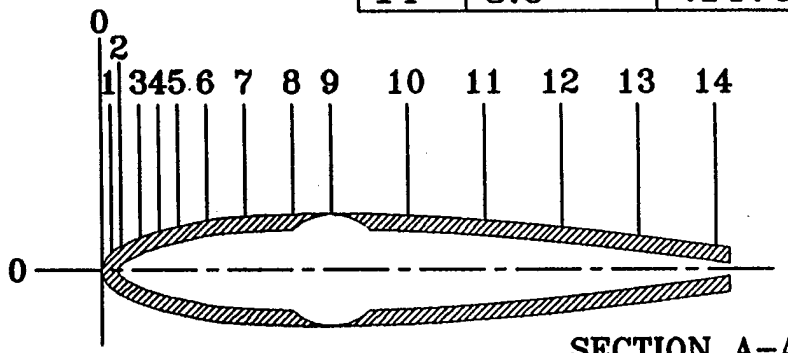

SECTION A–A

MATERIAL: 304 S.S. – .090 THK.

41

UNLESS OTHERWISE SPECIFIED DIMENSIONS ARE IN INCHES TOLERANCES DECIMALS ANGULAR .XX=+.015 −.015 +30' −30' .XXX=+.005 −.005 DO NOT SCALE DRAWING	CONTRACT NO.		THERMACORE INC.
	DRAWN EHD	DATE 3/23/96	TITLE: TYPE 1 HEAT PIPE–AIRFOIL SURFACE
TREATMENT	CHECKED		
FINISH	APPROVED J L Sanzi	4/11/96	SIZE A — DWG. NO. A–11–1324–3
SIMILAR TO / ACT. WT. / CALC. WT.	APPROVED		SCALE — RELEASE DATE — SHEET
	CUSTOMER		

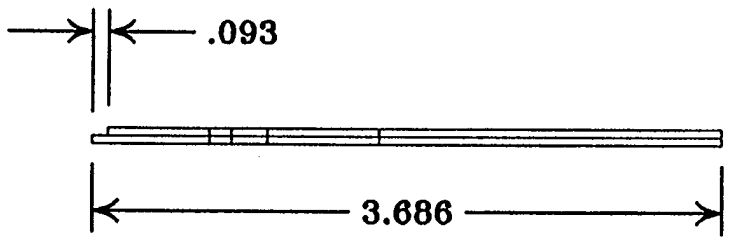

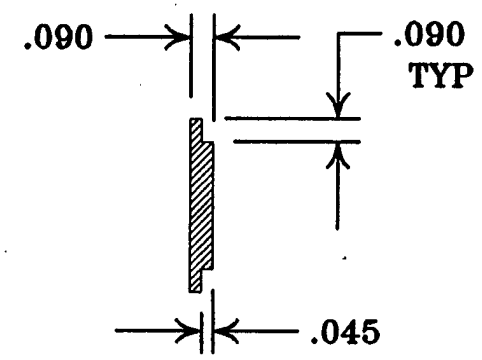

SECTION A-A

PT.	X	Y
1	.0563	.1065
2	.1125	.1471
3	.225	.1999
4	.3375	.2363
5	.45	.2634
6	.675	.3007
7	.9	.3227
8	1.125	.3342
9	1.35	.3376
10	1.8	.3264
11	2.25	.2978
12	2.7	.2567
13	3.15	.2061
14	3.6	.1476

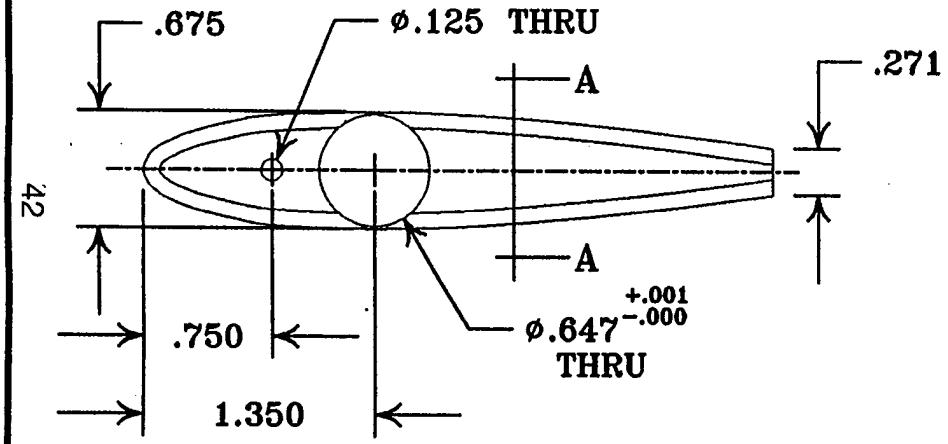

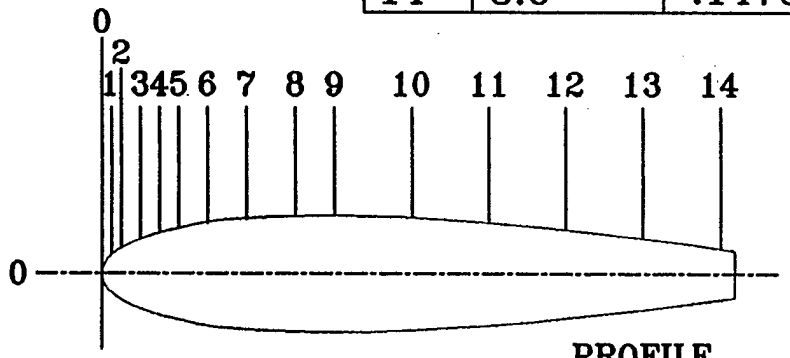

PROFILE

MATERIAL: 304 S.S.

UNLESS OTHERWISE SPECIFIED DIMENSIONS ARE IN INCHES TOLERANCES DECIMALS ANGULAR .XX=+.015 -.015 +30' -30' .XXX=+.005 -.005 DO NOT SCALE DRAWING	CONTRACT NO.		THERMACORE INC.
TREATMENT	DRAWN EHD	DATE 3/25/96	TITLE TYPE 1 HEAT PIPE- INBOARD END CAP
FINISH	CHECKED		
SIMILAR TO / ACT. WT. / CALC. WT.	APPROVED J L Sanzi	4/11/96	SIZE A / DWG. NO. A-11-1324-4
	APPROVED		SCALE — / RELEASE DATE / SHEET
	CUSTOMER		

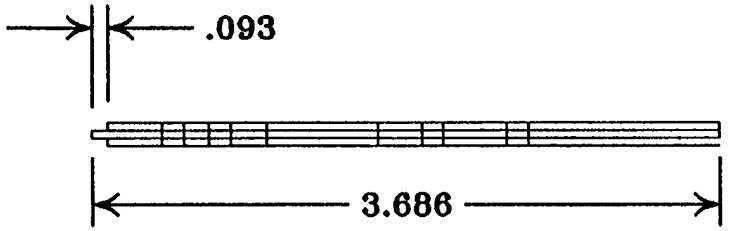

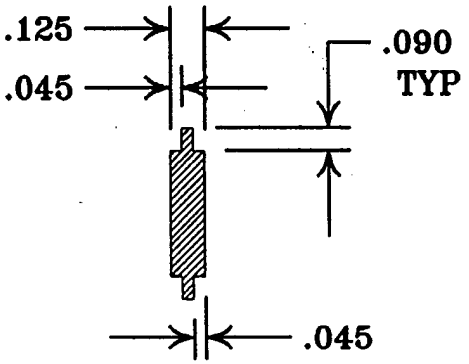

SECTION A-A

PT.	X	Y
1	.0563	.1065
2	.1125	.1471
3	.225	.1999
4	.3375	.2363
5	.45	.2634
6	.675	.3007
7	.9	.3227
8	1.125	.3342
9	1.35	.3376
10	1.8	.3264
11	2.25	.2978
12	2.7	.2567
13	3.15	.2061
14	3.6	.1476

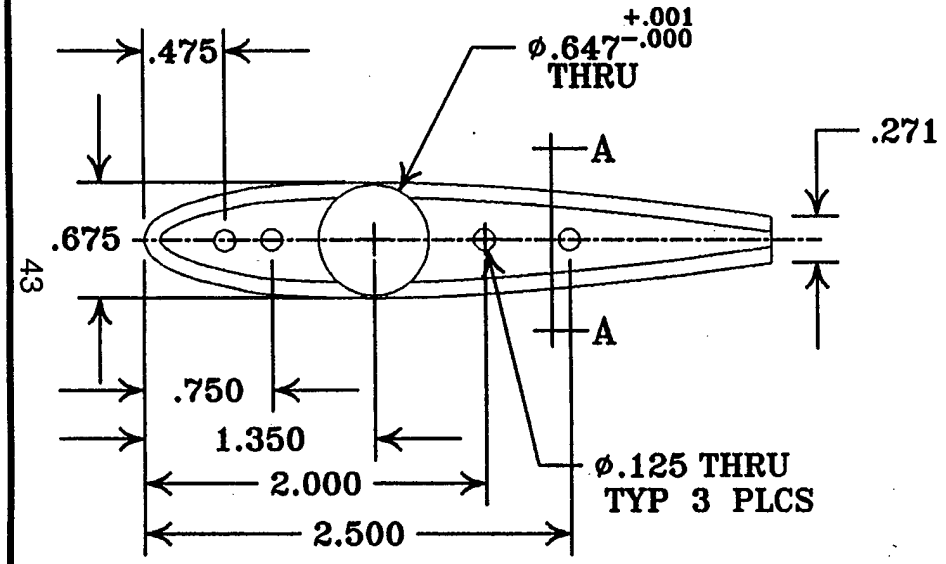

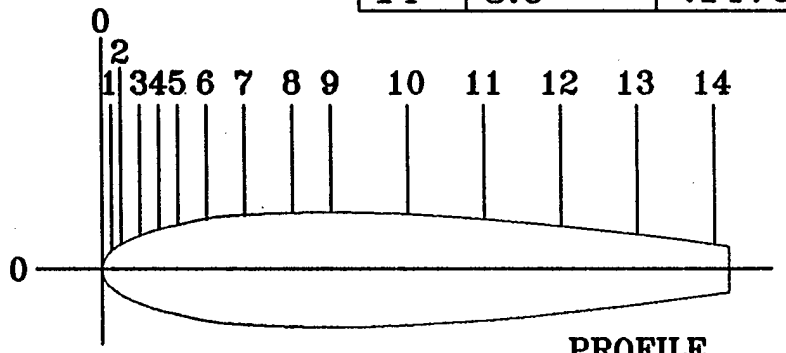

PROFILE

MATERIAL: 304 S.S.

UNLESS OTHERWISE SPECIFIED
DIMENSIONS ARE IN INCHES
TOLERANCES
DECIMALS ANGULAR
.XX=+.015 -.015 +30' -30'
.XXX=+.005 -.005 DO NOT SCALE DRAWING

TREATMENT

FINISH

SIMILAR TO | ACT. WT. | CALC. WT.

CONTRACT NO.

DRAWN EHD DATE 3\23\96

CHECKED

APPROVED J L Lanzi 4\11\96

APPROVED

CUSTOMER

THERMACORE INC.

TITLE
TYPE 1 HEAT PIPE-
DIVIDER

SIZE A | DWG. NO. A-11-1324-5

SCALE ——— | RELEASE DATE | SHEET

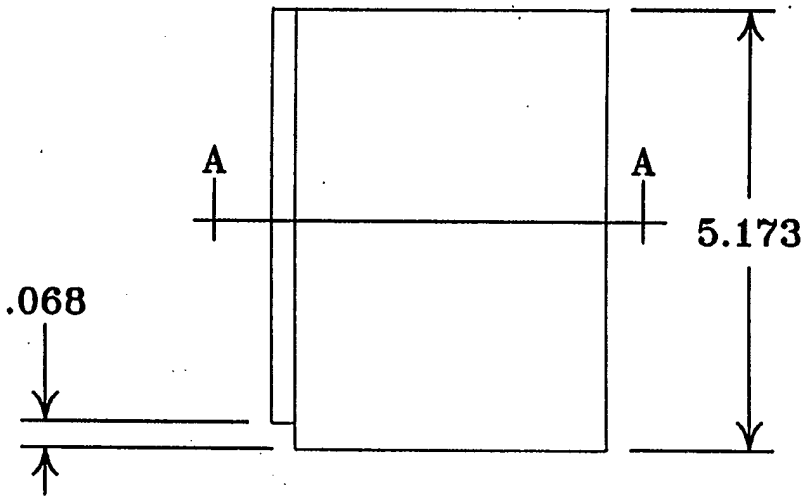

PT.	X	Y
1	−.125	.028
2	−.250	.049
3	−.375	.069
4	−.500	.089
5	−.625	.107
6	−.750	.126

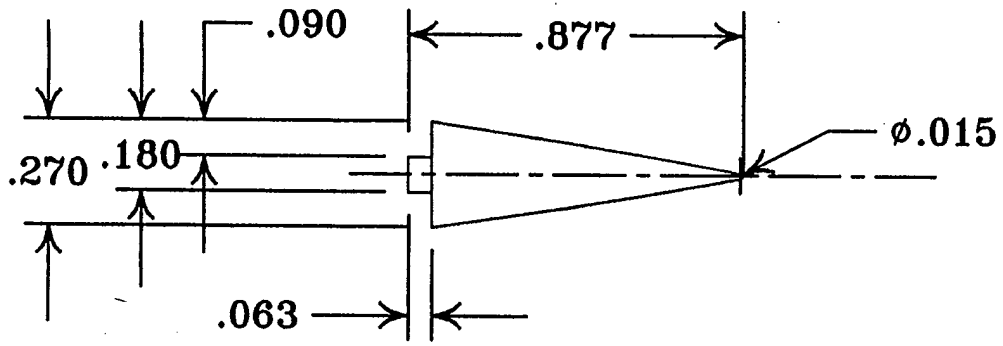

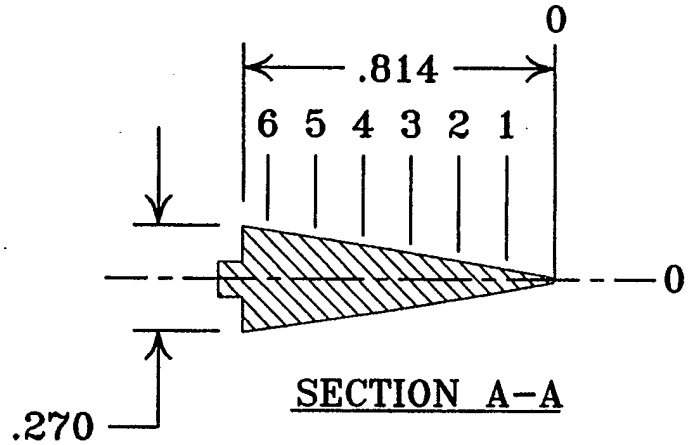

SECTION A-A

MATERIAL: 304 S.S.

44

UNLESS OTHERWISE SPECIFIED DIMENSIONS ARE IN INCHES TOLERANCES DECIMALS .XX=+.015 −.015 .XXX=+.005 −.005 ANGULAR +30' −30' DO NOT SCALE DRAWING	CONTRACT NO.		THERMACORE INC.
	DRAWN EHD	3\23\96	
TREATMENT	CHECKED		TITLE TYPE 2 WINGLET-TRAILING EDGE
FINISH	APPROVED J L Lenzi	4\11\96	
	APPROVED		SIZE A — DWG. NO. A-11-1324-6
SIMILAR TO — ACT. WT. — CALC. WT.	CUSTOMER		SCALE — RELEASE DATE — SHEET

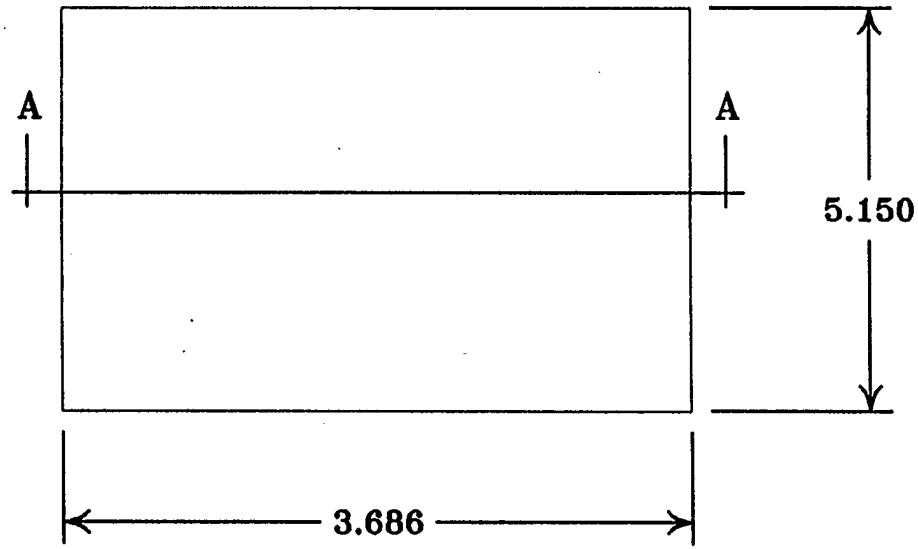

PT.	X	Y
1	.0563	.1065
2	.1125	.1471
3	.225	.1999
4	.3375	.2363
5	.45	.2634
6	.675	.3007
7	.9	.3227
8	1.125	.3342
9	1.35	.3376
10	1.8	.3264
11	2.25	.2978
12	2.7	.2567
13	3.15	.2061
14	3.6	.1476

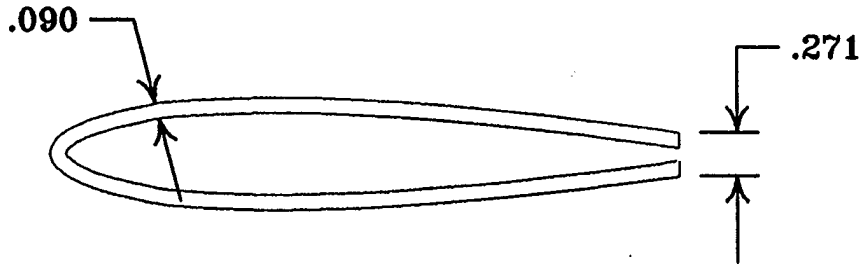

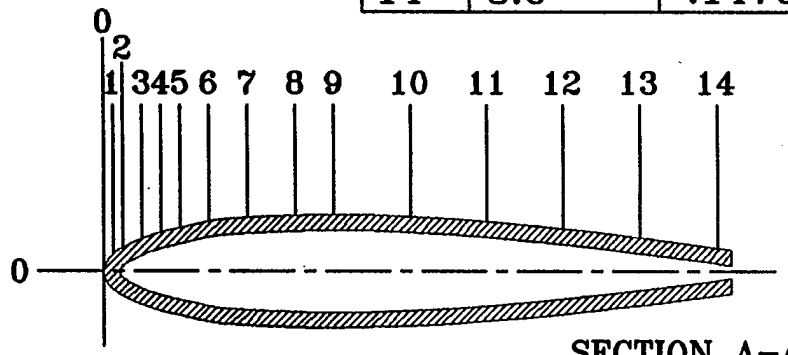

SECTION A–A

MATERIAL: 304 S.S. – .090 THK.

UNLESS OTHERWISE SPECIFIED
DIMENSIONS ARE IN INCHES
TOLERANCES
DECIMALS ANGULAR
.XX=+.015 –.015 +30' –30'
.XXX=+.005 –.005 DO NOT SCALE DRAWING

TREATMENT

FINISH

SIMILAR TO | ACT. WT. | CALC. WT.

CONTRACT NO.

DRAWN EHD DATE 3/23/96

CHECKED

APPROVED

APPROVED

CUSTOMER

THERMACORE INC.

TITLE

TYPE 2 WINGLET – AIRFOIL SURFACE

SIZE A

DWG. NO. A-11-1324-7

SCALE ——— RELEASE DATE SHEET

QUAN.	DIM "L"
1	2.0"
2	1.0"

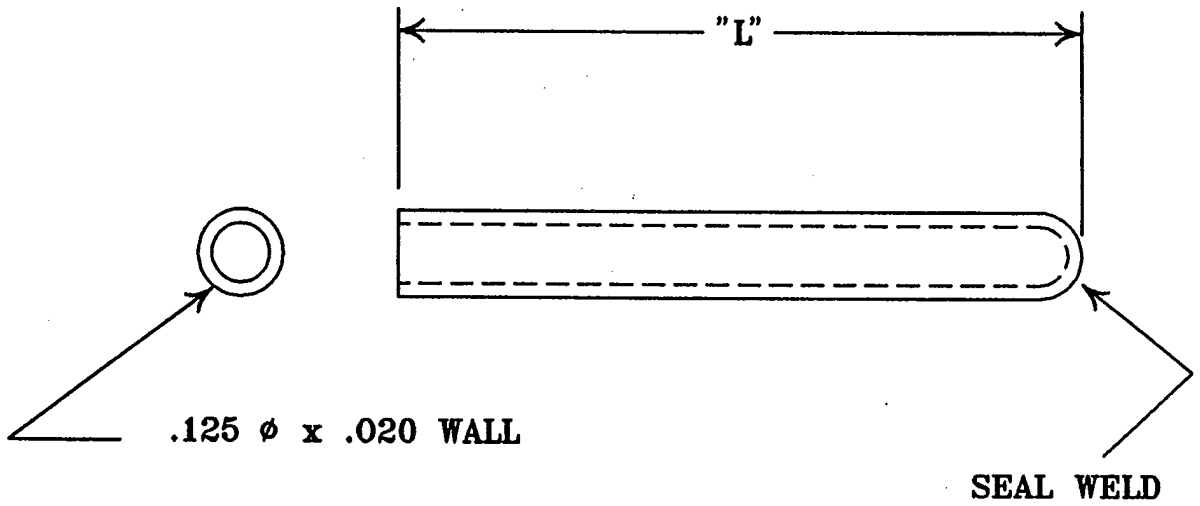

MATERIAL: 304 S.S.

UNLESS OTHERWISE SPECIFIED
DIMENSIONS ARE IN INCHES
TOLERANCES
DECIMALS ANGULAR
.XX=+.015 -.015 +30' -30'
.XXX=+.005 -.005 DO NOT SCALE DRAWING

TREATMENT

FINISH

SIMILAR TO | ACT. WT. | CALC. WT.

CONTRACT NO.

DRAWN EHD DATE 3/23/96

CHECKED

APPROVED

APPROVED

CUSTOMER

THERMACORE INC.

TITLE
TYPE 1 HEAT PIPE-
TC- TUBES

SIZE A

DWG. NO. A-11-1324-8

SCALE ——— RELEASE DATE SHEET

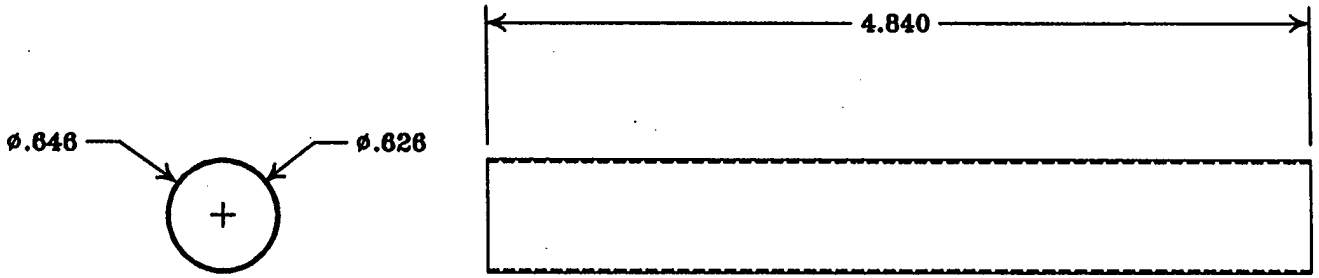

47

MATERIAL: 304 S.S.

UNLESS OTHERWISE SPECIFIED DIMENSIONS ARE IN INCHES TOLERANCES DECIMALS .XX=+.015 −.015 .XXX=+.005 −.005 ANGULAR +30' −30' DO NOT SCALE DRAWING	CONTRACT NO.		THERMACORE INC.
TREATMENT	DRAWN EHD	DATE 3/23/96	TITLE: ACUTATOR TUBE
FINISH	CHECKED		
	APPROVED		SIZE A — DWG. NO. A-11-1324-9
SIMILAR TO — ACT. WT. — CALC. WT.	APPROVED		SCALE ——— — RELEASE DATE — SHEET
	CUSTOMER		

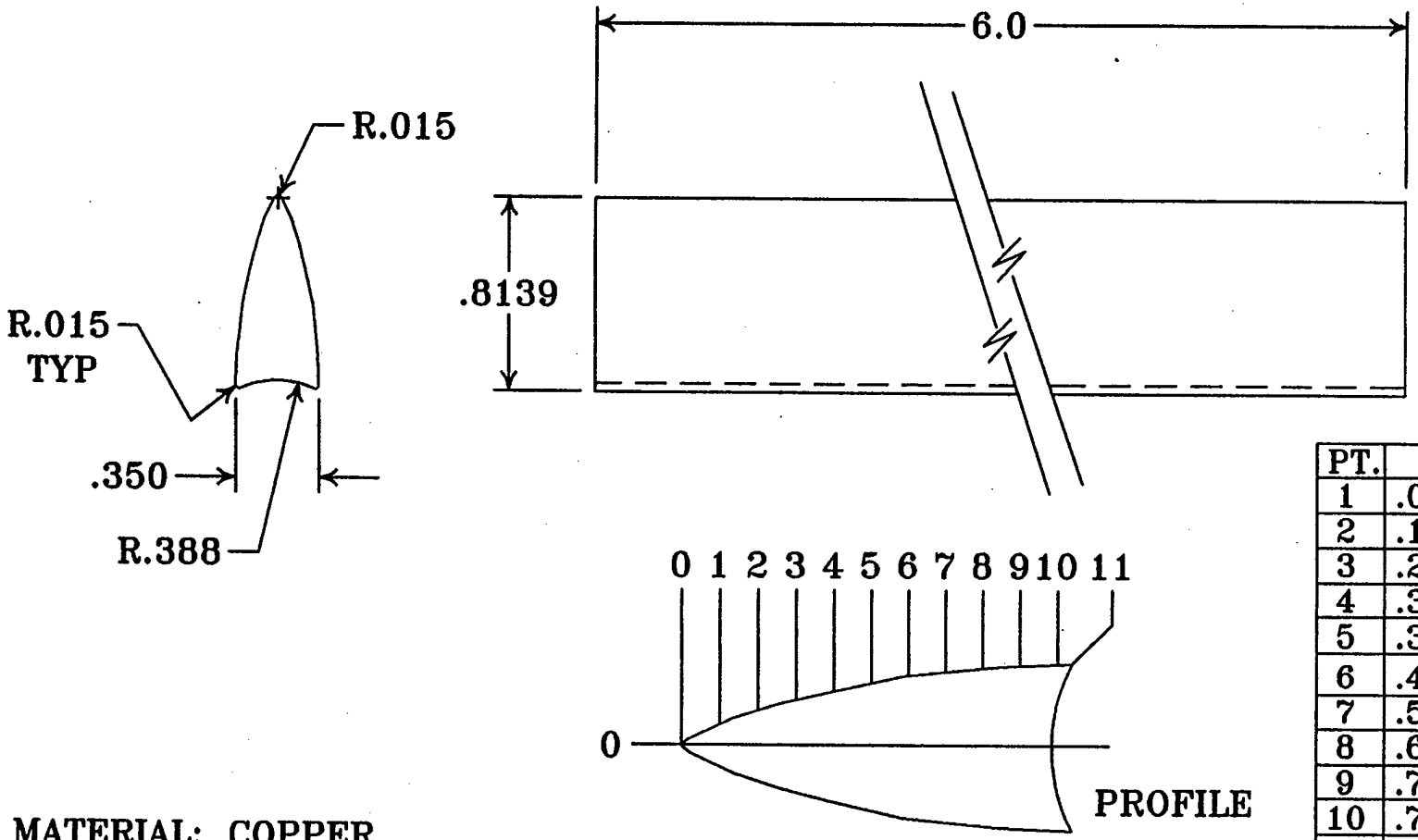

PT.	X	Y
1	.0782	.0407
2	.1582	.0707
3	.2382	.0937
4	.3182	.1128
5	.3982	.1305
6	.4782	.1469
7	.5582	.1547
8	.6382	.1626
9	.7182	.1682
10	.7982	.1715
11	.8288	.1727

MATERIAL: COPPER

48

UNLESS OTHERWISE SPECIFIED DIMENSIONS ARE IN INCHES TOLERANCES DECIMALS ANGULAR .XX=+.015 −.015 +30' −30' .XXX=+.005 −.005 DO NOT SCALE DRAWING	CONTRACT NO.	THERMACORE INC.
TREATMENT	DRAWN EHD DATE 3\15\96	TITLE TYPE 1 HEAT PIPE– FRONT WICK MANDREL
FINISH	CHECKED	
SIMILAR TO / ACT. WT. / CALC. WT.	APPROVED J L Sanzi 4\11\96	SIZE A / DWG. NO. A–11–1324–10
	APPROVED	SCALE ——— / RELEASE DATE / SHEET
	CUSTOMER	

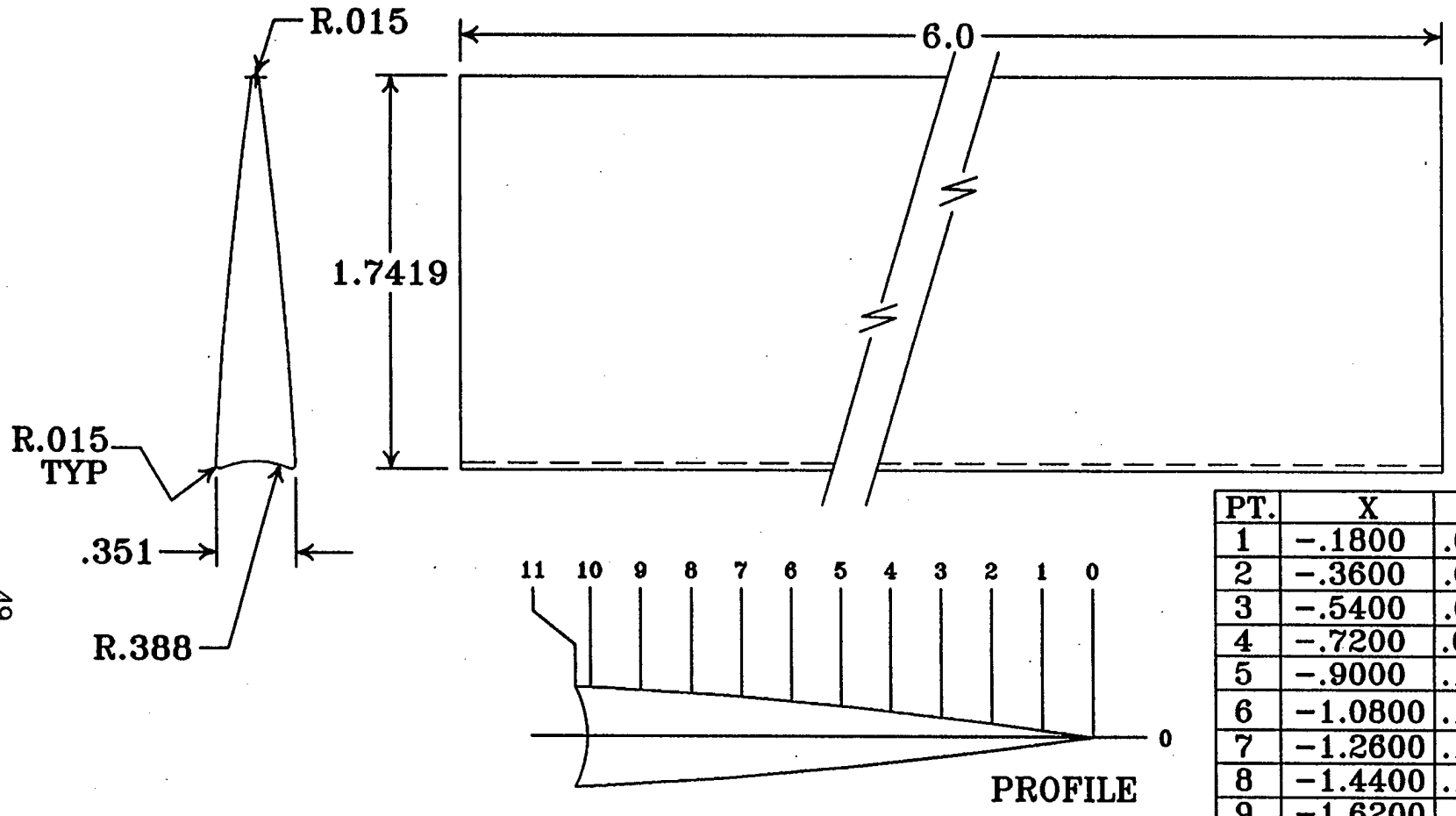

PT.	X	Y
1	−.1800	.0234
2	−.3600	.0468
3	−.5400	.0680
4	−.7200	.0883
5	−.9000	.1078
6	−1.0800	.1242
7	−1.2600	.1406
8	−1.4400	.1535
9	−1.6200	.1649
10	−1.8000	.1746
11	−1.8522	.1759

MATERIAL: COPPER

49

UNLESS OTHERWISE SPECIFIED
DIMENSIONS ARE IN INCHES
TOLERANCES
DECIMALS ANGULAR
.XX=+.015 −.015 +30' −30'
.XXX=+.005 −.005 DO NOT SCALE DRAWING

TREATMENT

FINISH

SIMILAR TO | ACT. WT. | CALC. WT.

CONTRACT NO.

DRAWN EHD DATE 3\15\96

CHECKED

APPROVED J L Lanzi 4\11\96

APPROVED

CUSTOMER

THERMACORE INC.

TITLE
TYPE 1 HEAT PIPE-
REAR WICK MANDREL

SIZE A

DWG. NO. A-11-1324-11

SCALE ——— RELEASE DATE SHEET

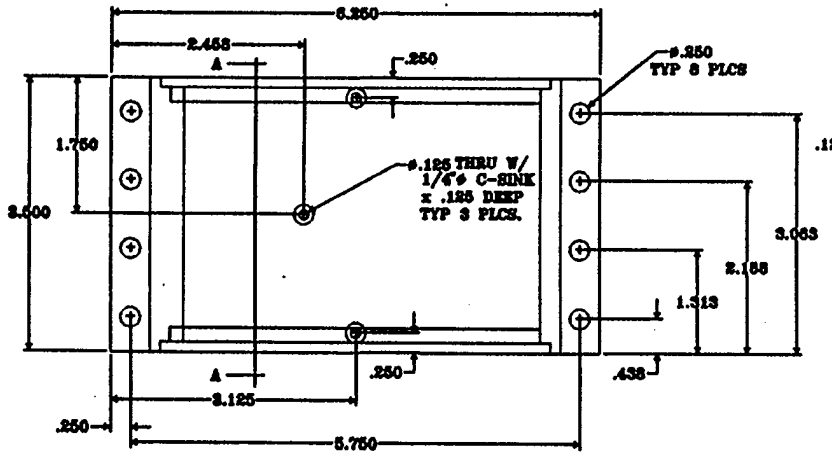

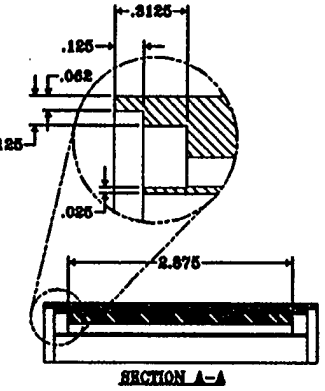

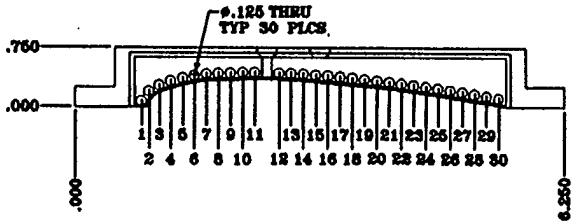

HOLE SCHEDULE

HOLE	"X"	"Y"
1	.847	.077
2	.942	.201
3	1.075	.278
4	1.222	.350
5	1.377	.368
6	1.528	.401
7	1.685	.429
8	1.838	.435
9	1.993	.429
10	2.148	.439
11	2.303	.441
12	2.613	.435
13	2.768	.428
14	2.923	.419
15	3.078	.409
16	3.234	.400
17	3.388	.384
18	3.543	.369
19	3.698	.353
20	3.853	.337
21	4.008	.319
22	4.163	.300
23	4.318	.280
24	4.473	.260
25	4.628	.238
26	4.783	.216
27	4.938	.193
28	5.093	.168
29	5.248	.143
30	5.403	.117

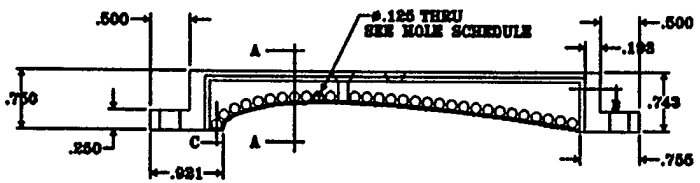

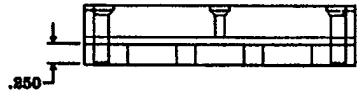

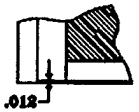

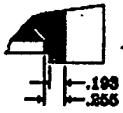

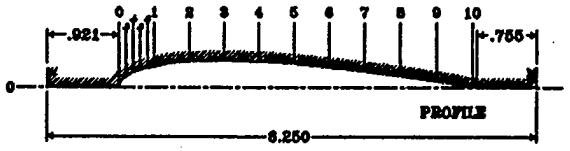

PROFILE POINTS

PT.	X	Y
.2	.0904	.1379
.4	.1808	.1885
.6	.2712	.2239
.8	.3616	.2509
1	.4523	.2726
2	.9044	.3303
3	1.3566	.3484
4	1.8088	.3376
5	2.2610	.3089
6	2.7132	.2676
7	3.1654	.2170
8	3.6176	.1585
9	4.0698	.0912
10	4.5232	.0164

MATERIAL: 304 S.S.

50

REVISIONS			
LTR.	DESCRIPTION	DATE	APPROVED

UNLESS OTHERWISE SPECIFIED
DIMENSIONS ARE IN INCHES
TOLERANCES
DECIMALS ANGULAR
.XX=+.015 -.015 +30' -30'
.XXX=+.005 -.005 DO NOT SCALE DRAWING

TREATMENT

FINISH

SIMILAR TO | ACT. WT. | CALC. WT.

CONTRACT NO.

DRAWN EHD 5/21/98

CHECKED

APPROVED J L Lanzi 6/11/98

APPROVED

CUSTOMER

THERMACORE INC.

TITLE
HEAT PIPE - CALORIMETER

SIZE B

DWG. NO. B-11-1324-13

SCALE —— RELEASE DATE SHEET

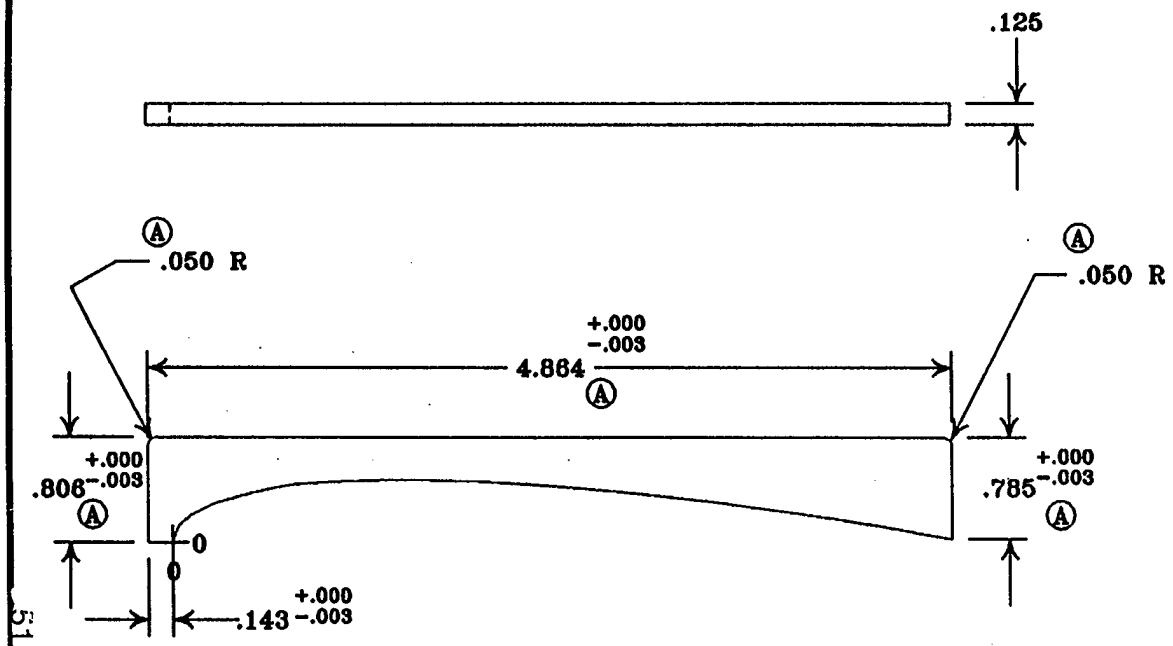

PT.	X	Y
1	.0563	.1123
2	.1125	.1561
3	.225	.2133
4	.3375	.2523
5	.45	.2803
6	.675	.3185
7	.90	.3448
8	1.125	.3573
9	1.35	.3614
10	1.80	.3520
11	2.25	.3247
12	2.70	.2844
13	3.15	.2345
14	3.60	.1767
15	4.05	.1112
16	4.50	.0376
17	4.5975	.0205

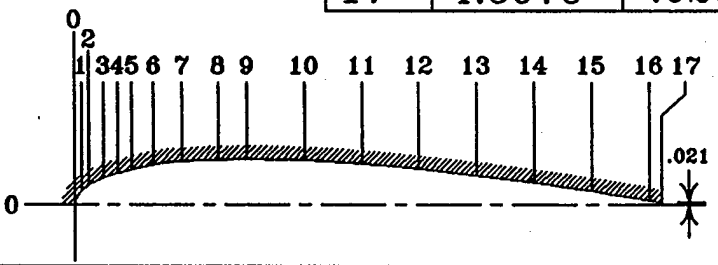

MATERIAL: 304 S.S. – .125 THK.

REV	A	4\24\96	4.864W4.740,.896W.613,.785W.592, ADDED RADIUS NOTE

UNLESS OTHERWISE SPECIFIED
DIMENSIONS ARE IN INCHES
TOLERANCES
DECIMALS ANGULAR
.XX=+.015 −.015 +30' −30'
.XXX=+.005 −.005 DO NOT SCALE DRAWING

TREATMENT

FINISH

SIMILAR TO | ACT. WT. | CALC. WT.

CONTRACT NO.

DRAWN EHD DATE 3\25\96

CHECKED

APPROVED J L Lanzi 4\11\96

APPROVED

CUSTOMER

THERMACORE INC.

TITLE

CALORIMETER END CAP

SIZE		DWG. NO.	REV
A		A-11-1324-14	A

SCALE ——— | RELEASE DATE | SHEET

Appedix C:

Methematica Program for Transient Model

```
(*  This workbook calculates the transient response
    of a Na missile-fin heat pipe based a lumped
    capacitance model of continuum front propagation.

    Front Heat Pipe (leading edge).                    *)


(* constants used in claculation *)

tempvalue = {{0.0, 300.0}};
zvalue = {{0.0, 0.0}};

ze = 0.050;  (* evaporator length, m *)
zc = 0.056;  (* condenser length, m *)
thp = 300.0;   (* current heat pipe temperature, K *)
tmelt = 371.0;  (* melting temperature of Na, K *)
time = 0.0;   (* current time, s *)
dtime = 0.1;   (* time increment, s *)
ap = 0.0001145;  (* perimeter by thickness of pipe wall, m2 *)
aw = 0.000050;   (* perimeter by thickness of wick, m2 *)
ae = 0.0025;   (* perimeter by evaporator length, m2 *)
eps = 0.55;   (* porosity of the wick, non-dimensional *)
r = 361.478;   (* R, gas constant, for Na *)
gamma = 1.67;   (* specific heat ratio for Na *)
l = 0.015;    (* characteristic length for mean-free-path, m *)
av = 0.00020;    (* area of vapor section, m2 *)
he = 752.0;   (* convection constant for evaporator, W/m2-K *)
hc = 550.0;    (* convection constant for condenser, W/m2-K *)
ter = 1213.0;   (* heat source temperature, K *)
tinf = 327.0;    (* heat sink temperature, K *)
p = 0.05;     (* perimeter of heat pipe, m2 *)
zn = 0.0;   (* initial continuum front position, m *)

hsl = 113000.0;   (* heat of fusion for Na, J/kg *)


(* temperature dependant functions *)

qe[t_] := he ae (ter - t)  (* W *)

hfg[t_] := (5.335 (10^6) - 4185.8 t + 9.097 t^2 - 1.1117*(10^-2) t^3
            + 6.2049 (10^-6) t^4 - 1.2942 (10^-9) t^5)  (* J/kg *)

rhoss[t_] := 8055.0  (* kg/m3 *)

rhoni[t_] := 8900.0  (* kg/m3 *)

rhos[t_] := 1033.45 - 0.221268 t  (*kg/m3 *)

rhol[t_] := (991.42 - 8.8062 (10^-2) t - 3.4209 (10^-4) t^2
             + 3.7279 (10^-7) t^3 - 1.9426*(10^-10) t^4
             + 3.8804 (10^-19) t^5)  (* kg/m3 *)

rhov[t_] := Exp[-86.67 + 0.3067 t - 4.972*(10^-4) t^2
                + 4.323*(10^-7) t^3 - 1.925*(10^-10) t^4
                + 3.443*(10^-14) t^5]  (* kg/m3 *)

cpss[t_] := 372.115 + 0.421348 t - 0.000188779 t^2 (*J/kg-K *)

cpni[t_] := 235.0 + 0.863643 t - 0.000551786 t^2 (*J/kg-K *)
```

```
cpsodl[t_] := 1550.0 - 0.564899 t + 0.000274368 t^2  (*J/kg-K *)

cpsods[t_] := 1364.2  (* J/kg-K *)

muv[t_] := (6.8708 (10^-6) + 2.506 (10^-8) t - 3.6443 (10^-11) t^2
            + 4.9847 (10^-14) t^3 - 3.217 (10^-17) t^4
            + 7.6982 (10^-21) t^5)  (* N-s/m2 *)

qs[t_] := av rhov[t] hfg[t] Sqrt[0.5 gamma r t/(gamma + 1)] (* W *)

c1[t_] := (rhoss[thp] cpss[thp] ap + (1. - eps) (rhoni[thp] cpni[thp] aw)
           + eps rhos[thp] cpsods[thp] aw)  (* J/m-K *)

c2[t_] := (rhoss[thp] cpss[thp] ap + (1. - eps) (rhoni[thp] cpni[thp] aw)
           + eps rhol[thp] cpsodl[thp] aw)  (* J/m-K *)

(* stage 1 *)

While[ (* test *) thp < tmelt,
   (* body *)

   thpnew = thp + (qe[thp] dtime)/(c1[thp] ze);

   thp = thpnew;

   time = time + dtime;

   AppendTo[tempvalue, {time, thp}];
   AppendTo[zvalue, {time, zn}];

   (* end of While loop *) ];

Print[time, " s  for the evaporator to reach melt temp."]
Print[thp, " K  is the current evaporator temperature."]

(* end of stage 1 *)


1.3 s  for the evaporator to reach melt temp.
373.76 K  is the current evaporator temperature.


(* stage 2 - melting evaporator *)

dtimemelt = eps rhol[500.0] aw ze hsl/qe[thp];

time = time + dtimemelt;

Print[time, " s  to thaw evaporator section."]
Print[thp, " K  is the current evaporator temperature."]

AppendTo[tempvalue, {time, thp}];
AppendTo[zvalue, {time, zn}];

(* end of stage 2 *)


1.38827 s  to thaw evaporator section.
373.76 K  is the current evaporator temperature.
```

```
(* stage 3 *)

(* first find transition temperature, tt *)

tt = x /. FindRoot[x == 5020.0 Pi (muv[x]/(rhov[x] 1))^2.0,
                   {x, 600.0}];


(* iterate untill tt is reached *)

While[ (* test *) thp < tt,
   (* body *)

   thpnew = thp + (qe[thp] dtime)/(c2[thp] ze);

   thp = thpnew;

   time = time + dtime;

   AppendTo[tempvalue, {time, thp}];
   AppendTo[zvalue, {time, zn}];

   (* end of While loop *) ];

Print[tt, " K  is the transition temperature."]
Print[time, " s  to reach transition temperature."]
Print[thp, " K  is the current evaporator temperature."]

(* end of stage 3 *)


832.091 K  is the transition temperature.
15.1883 s  to reach transition temperature.
832.717 K  is the current evaporator temperature.
```

```
(* stage 4 *)

dtime = 10.0 dtime;

zn = ze;
znew = ze;
zold = 0.0;

(* iterate untill zn = ze+zc or steady-state is reached *)


While[ (* test *) znew < (ze + zc)  &&  Abs[zn - zold] > 0.000001,
   (* body *)

   {thpnew, qf} = {xx, yy} /. FindRoot[
                  {qe[thp] == hc p (zn - ze) (thp - tinf) + yy
                              + c2[thp] zn (xx - thp)/dtime,
                   yy == Min[qe[thp], qs[thp]] - hc p (zn - ze) (thp - tinf)
                           - c2[thp] (zn - ze) (xx - thp)/dtime},
                  {xx, 800.0}, {yy, 999.0}];  (* K, and W *)

   znew = zn + qf dtime/(rhol[500.0] eps aw hsl + c1[350.0] (tmelt
          - tinf) + c2[700.0] (thpnew - tmelt));  (* m *)

   thp = thpnew;

   zold = zn;

   zn = znew;

   If[Abs[zn - zold] <= 0.000001, Print["steady-state reached at"]];

   time = time + dtime;

   AppendTo[tempvalue, {time, thp}];
   AppendTo[zvalue, {time, zn}];

   (* end of While loop *) ];


Print[time, " s  after startup."]
Print[thp, " K  is the heat pipe temperature."]
Print[zn, " m  is the continuum front location."]

(* end stage 4 *)


steady-state reached at
205.188 s  after startup.
832.717 K  is the heat pipe temperature.
0.101383 m  is the continuum font location.
```

```
(* stage 5 *)

(* iterate untill steady state is reached *)

thpnew = tinf;
thpold = tinf - 10.0;

While[ (* test *) N[thpold, 4] != N[thpnew, 4],
   (* body *)

   thpnew = thp + (qe[thp] - hc p zc (thp - tinf)) dtime/(c2[thp] (ze + zc));

   thpold = thp;

   thp = thpnew;

   time = time + dtime;

   AppendTo[tempvalue, {time, thp}];
   AppendTo[zvalue, {time, zn}];

   (* end of While loop *) ];

Print["Steady-state reached at"]
Print[time, " s  after startup."]
Print[thp, " K  is the heat pipe temperature."]

(* end stage 5 *)
```

```
1.

Steady-state reached at
585.488 s  after startup.
814.041 K  is the heat pipe temperature.
```

```
ListPlot[Take[tempvalue,250]]
ListPlot[Take[zvalue, 250]]
ListPlot[tempvalue]
ListPlot[zvalue]
```

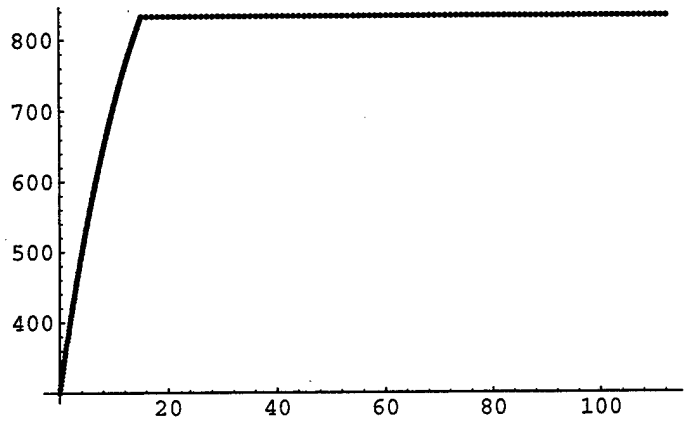


```
-Graphics-
```

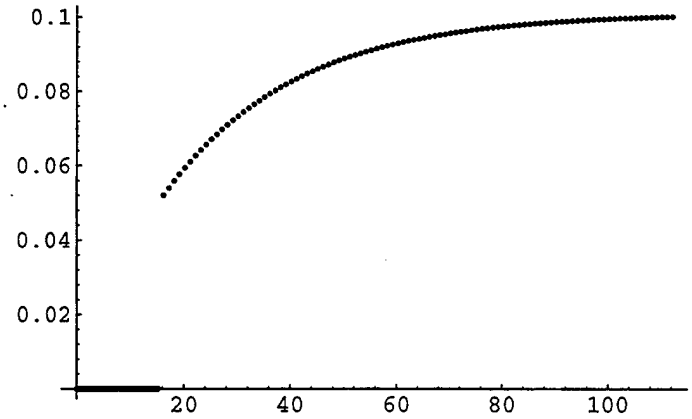

-Graphics-

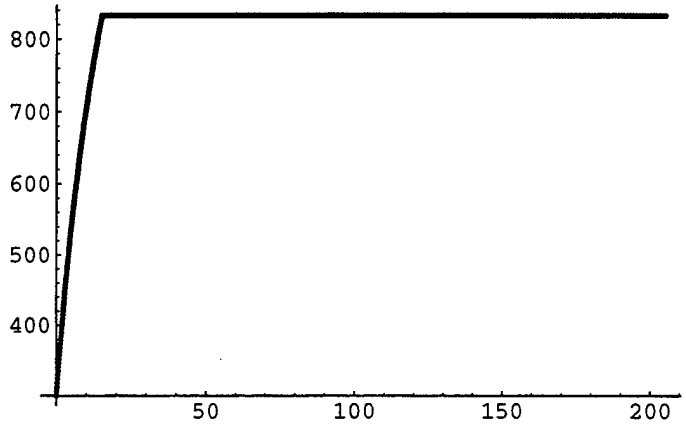

-Graphics-

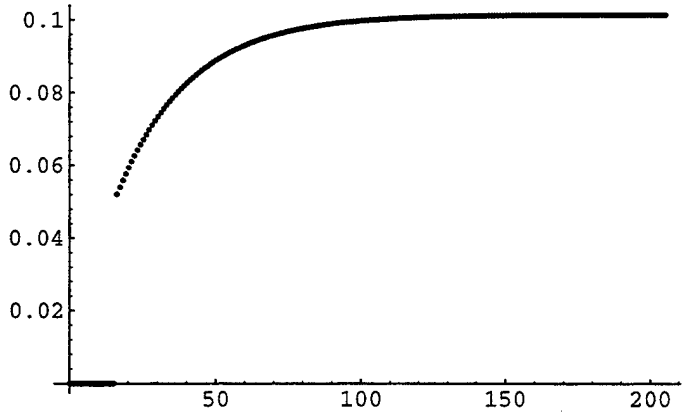

-Graphics-